Article

Development and Validation of a Parameter-Free Model Chemistry for the Computation of Reliable Reaction Rates

Vincenzo Barone,* Jacopo Lupi, Zoi Salta, and Nicola Tasinato

Read Online

ACCESS | Metrics & More | Article Recommendations | Supporting Information

ABSTRACT: A recently developed model chemistry (jun-Cheap) has been slightly modified and proposed as an effective, reliable, and parameter-free scheme for the computation of accurate reaction rates with special reference to astrochemical and atmospheric processes. Benchmarks with different sets of state-of-the-art energy barriers spanning a wide range of values show that, in the absence of strong multireference contributions, the proposed model outperforms the most well-known model chemistries, reaching a subchemical accuracy without any empirical parameter and with affordable computer times. Some test cases show that geometries, energy barriers, zero point energies, and thermal contributions computed at this level can be used in the framework of the master equation approach based on the ab initio transition-state theory for obtaining accurate reaction rates.
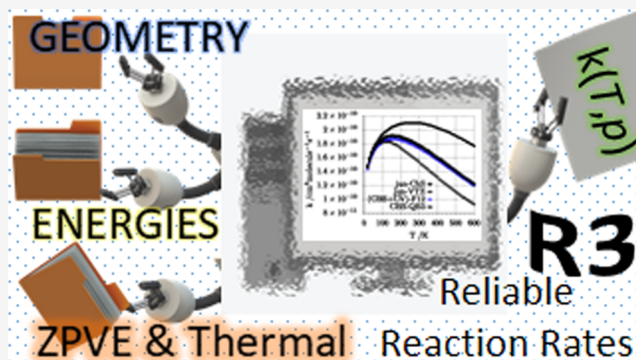
■ INTRODUCTION

For many years, scientists were skeptical about the presence of molecular systems in the interstellar space due to the harsh physical conditions (low temperature and pressure in the presence of high-energy radiation fields) characterizing this environment. However, contrary to these expectations, more than 200 molecules have now been identified in the interstellar and circumstellar medium (ISM),[1] including several so-called interstellar complex organic molecules (iCOMs), namely, molecules containing carbon and a total of more than six atoms.[2] Most of the observed species should have a very short lifetime according to Earth-based standards, but the intermolecular processes leading to thermodynamic equilibrium are not effective in the ISM due to its extreme physical parameters.[3,4] This situation calls for a strong interplay among observations, laboratory studies, and computational approaches to understand the chemical evolution in these regions and to explain the observed abundances of different species.

Astrochemical models are virtual laboratories including thousands of reactions and whose main goal is to reproduce the observational data to the best possible extent. Although the available astrochemical models show widely different degrees of sophistication,[5] all of them share the same basic ingredients:[6] a set of initial conditions (total density, temperature, etc.) and a panel of chemical reactions characterized by their respective temperature-dependent rate constants and most likely exit channels. To improve the current predictions provided by these models, the reactions responsible for the largest uncertainties on the abundances must be studied in more detail by laboratory experiments and/ or theoretical methods to provide improved rate constants and branching ratios.

Chemical kinetics plays a fundamental role also in the different but related context of atmospheric models that try to reproduce and interpret the large number of chemical processes occurring in the troposphere and stratosphere. Reaction rate coefficients and product yields have been either traditionally obtained by means of suitable experimental techniques[7] or estimated using structure—activity relationships.[8] The massive number of organic compounds released in the atmosphere and the corresponding huge number of possible reactions ruling their oxidation/degradation pathways make experimental measurements of even a small fraction of key processes a daunting task. In recent years, computational chemistry has begun to contribute substantially to a better understanding of several important reaction sequences in the atmosphere.[9] These contributions have, at their heart, the use of electronic structure calculations to determine the energies and other characteristics (mainly geometries and vibrational frequencies) of stable species, reactive complexes, and transition states, which are then used in theoretical frameworks

to determine rate coefficients. The main factor limiting the accuracy of this process is the computation of accurate values for all of the energy barriers ruling the different elementary steps. Next, zero point energies (ZPEs) and finite temperature contributions (FTCs) come into play, whose contributions may become non-negligible already for medium-sized systems.

Several nonempirical procedures have been developed and employed for the generation of accurate thermochemical data, which for small systems come close to the full configuration interaction (FCI) complete basis set (CBS) limit.[10] Among the most successful approaches are the Weizmann-n series (with the most accurate being W4[11]), the focal point analysis (FPA),[12,13] the Feller−Dixon−Peterson model (FDP),[14] and the extrapolated ab initio thermochemistry (HEAT) protocol.[15−17] A simplified version of the HEAT protocol is obtained by retaining only the extrapolation to the CBS limit at the CCSD(T) level and incorporating the core-valence corrections, thus leading to the model referred to in the following as CBS-CV. This approach is rather well tested in the literature and was shown to provide results with an accuracy well within 0.5 kcal mol^{-1}. Recently, alternative protocols have been proposed, which employ explicitly correlated approaches:[10,18] thanks to the faster convergence to the complete basis set limit, these approaches allow some computer time saving, but the rate-determining step remains the evaluation of higher-level contributions.

For larger molecular systems, more approximate composite methods are unavoidable, which aim at reaching the so-called chemical accuracy (1 kcal mol^{-1}). The most well-known among these so-called model chemistries are the last versions of the Gn[19] (G4[20]) and CBS-x[21] (CBS-QB3[22]) families. However, all of these models include some empirical parameters and employ geometries, which are not fully reliable for transition states and noncovalent complexes ruling the entrance channels of most reactions of astrochemical and atmospheric interest. As a matter of fact, the most reliable protocols (e.g., HEAT) push geometry optimizations to the limit to obtain accurate energetics, whereas, at the other extreme, Gn and CBS-x schemes employ B3LYP geometries, whose accuracy is often unsatisfactory.[23]

In the last few years, a reliable and accurate computational protocol, referred to as the cheap scheme (ChS) and devoid of any empirical parameter, has been developed and tested with remarkable success for structural and energetic data.[24−26] In conjunction with geometries and harmonic frequencies issuing from double-hybrid functionals, ChS has given promising results also for the activation energies of some reactions of astrochemical interest.[27−31] More recently, an improved variant (referred to as the jun-Cheap scheme, jChS) has been introduced, which, thanks to the use of the "june" partially augmented basis set of the "calendar" family,[32] provides very accurate results also for noncovalent interactions.[33,34] On these grounds, in this paper, we provide a comprehensive benchmark of the jChS model chemistry for several classes of reactions for which accurate reference results are available or have been purposely computed. Together with electronic energies, we analyze also zero point energies, thermal contributions to enthalpies and entropies, and overall reaction rates computed for elementary reactions in the framework of the master equation (ME) approach based on the ab initio transition-state theory (AITSTME).[35−37]

The paper is organized as follows. In the first part, we validate the jChS model chemistry with reference to some well-known databases: (i) the 24 energy barriers available in the latest updated version of the DBH24 database,[38] (ii) the 52 barriers of Truhlar's HTBH38[39] and NHTBH38[40] databases not included in DBH24, and (iii) seven representative reactions from Karton's BH28 database.[41] When needed, the reference values are updated by new computations performed with a composite method closely resembling the W3.2 model.[42]

Next, the reliability of the jChS model chemistry for zero point energies and thermal contributions to enthalpies and entropies is assessed with respect to the new databases THCS21 and THOS10 containing accurate reference values for closed- and open-shell systems, respectively.

Finally, the role of different contributions in determining the overall accuracy of computed reaction rates is analyzed by means of some simple elementary reactions and two more complex reaction networks relevant for astrochemistry and atmospheric chemistry. Conclusions and perspectives are given in the last section.

■ COMPUTATIONAL DETAILS

All of the composite schemes employed in the present work extrapolate single-point energies computed at suitable geometries (see next sections) using the cc-pV($n + d$)Z (hereafter nZ)[43] or jun-cc-pV($n + d$)Z (hereafter jnZ)[32] families of basis sets. The coupled cluster (CC) ansatz including single, double, and (perturbative) triple excitations (CCSD(T))[44] within the frozen-core approximation and in conjunction with 3Z or j3Z basis sets is always employed in the first step. Next, CBS extrapolation and core-valence correlation (CV) are added using either MP2[45] (leading, in conjunction with jnZ basis sets, to our standard jChS model) or CCSD(T). In the latter case, inclusion of higher-level terms (diagonal Born−Oppenheimer,[46−49] scalar relativistic,[50,51] full triple and perturbative quadruple excitations[52−54]) and systematic use of nZ basis sets lead to the CBS-CVH scheme.

The effect of spin−orbit coupling is added to the energies of the O, OH, SH, and Cl radicals, lowering their electronic energies by 0.22, 0.20, 0.54, and 0.84 kcal mol^{-1}, respectively.[55]

Vibrational contributions are always obtained by the rev-DSDPBEP86-D3(BJ) double-hybrid functional,[56] in conjunction with the j3Z basis set (hereafter rev-DSD). Harmonic frequencies are computed by analytical second derivatives[57] and anharmonic corrections, when needed, by the generalized second-order vibrational perturbation theory (GVPT2) employing third- and semidiagonal fourth derivatives obtained by numerical differentiation of second derivatives implemented by one of the present authors in Gaussian software.[58−60]

All of the computations have been performed with the Gaussian code,[60] except for CCSD(T) geometry optimizations that have been carried out with the Molpro package,[61] CCSDT or CCSDT(Q) energy evaluations with the MRCC program,[62] and DBOC together with relativistic computations with the CFOUR code.[63]

jChS Model Chemistry. The jChS total electronic energies are obtained by single-point computations at rev-DSD geometries

$$E_{jChS} = E(CCSD(T)/j3Z) + \Delta E_{MP2}^{CBS} + \Delta E_{CV} \qquad (1)$$

where the CBS term is

Table 1. Theoretical Values of Barrier Heights in the DBH24/08 Data Set Obtained at Different Levels of Theory[e]

	reactions	forward/reverse barrier height			
		CCSD(T)	jChS	jChS[a]	ref[b]
			Heavy-Atom Transfer		
a1[c]	$H^\bullet + N_2O \rightarrow OH^\bullet + N_2$	17.89/84.96	17.53/83.25	17.58/83.27	17.13/82.47
a2	$H^\bullet + ClH \rightarrow HCl + H^\bullet$	18.89/18.89	17.31/17.31	17.33/17.33	18.00/18.00
a3[c]	$CH_3^\bullet + FCl \rightarrow CH_3F + Cl^\bullet$	7.21/62.20	7.16/60.37	7.05/60.28	6.75/60.00
			Nucleophilic Substitution		
a4	$Cl^- \cdots CH_3Cl \rightarrow ClCH_3 \cdots Cl^-$	13.56/13.56	13.26/13.26	13.28/13.28	13.41/13.41
a5	$F^- \cdots CH_3Cl \rightarrow FCH_3 \cdots Cl^-$	3.52/29.47	3.39/29.09	3.41/29.09	3.44/29.42
a6	$OH^- + CH_3F \rightarrow HOCH_3 + F^-$	−2.39/17.78	−2.48/17.36	−2.51/17.35	−2.44/17.66
			Unimolecular and Association		
a7	$H^\bullet + N_2 \rightarrow HN_2^\bullet$	15.23/11.01	14.34/11.12	14.36/11.09	14.36/10.61
a8	$H^\bullet + C_2H_4 \rightarrow C_2H_5^\bullet$	2.43/42.59	1.9/42.19	1.92/42.21	1.72/41.75
a9	$HCN \leftrightarrow HNC$	47.45/32.77	47.98/33.24	48.02/33.28	48.07/32.82
			Hydrogen Transfer		
a10[d]	$OH^\bullet + CH_4 \rightarrow CH_3^\bullet + H_2O$	7.05/19.05	6.63/20.04	6.52/19.94	6.71/19.60
a11[c,d]	$H^\bullet + OH^\bullet \rightarrow H_2 + {}^3O$	10.38/14.62	11.51/13.77	11.42/13.78	10.71/13.12
a12[c]	$H^\bullet + H_2S \rightarrow H_2 + HS^\bullet$	4.23/19.23	3.7/17.94	3.69/17.96	3.62/17.33
	MAX	2.49	0.80	0.80	
	MUE	0.71	0.36	0.35	
	RMSD	0.97	0.44	0.43	

[a]At QCISD/MG3 geometries. [b]Ref 38. [c]Spin−orbit contributions on the reverse reaction barrier. [d]Spin−orbit contributions on the forward reaction barrier. [e]All of the values (exclusive of ZPE) are in kcal mol^{-1}.

$$\Delta E_{MP2}^{CBS} = \frac{4^3 E(MP2/j4Z) - 3^3 E(MP2/j3Z)}{4^3 - 3^3} - E(MP2/j3Z) \tag{2}$$

and the core-valence correction ΔE_{CV} is the MP2 energy difference between all electron (ae) and frozen-core (fc) calculations employing the cc-pwCVTZ basis set.[64] At this level, the extrapolation of Hartree−Fock (HF) and correlation contributions is performed with the same equation and basis sets since several tests have shown that this simplified recipe has a negligible impact on the overall accuracy of the results. Furthermore, scalar relativistic effects are neglected, which is not a serious approximation since the heaviest element involved in this study is Cl.

CBS-CVH Composite Scheme. The CBS-CVH total electronic energies are obtained from single-point computations at geometries optimized by the jChS composite method described above for energies

$$E_{tot} = E_{HF}^{CBS} + \Delta E_{CCSD(T)}^{CBS} + \Delta E_{CV} + \Delta E_{fT} + \Delta E_{pQ}$$
$$+ \Delta E_{rel} + \Delta E_{DBOC} \tag{3}$$

In this case, HF and correlation energies are extrapolated separately. In particular, the HF CBS limit is estimated using Feller's exponential formula[65]

$$E_{HF}(n) = E_{HF}^{CBS} + B \exp(-Cn) \tag{4}$$

whereas the CBS limit of the correlation energy is obtained by the n^{-3} formula proposed by Helgaker and co-workers[66]

$$\Delta E_{corr}(n) = \Delta E_{corr}^{CBS} + An^{-3} \tag{5}$$

The three-point extrapolation of HF energies employs 3Z, 4Z, and 5Z basis sets, whereas the two smaller basis sets are used in the two-point extrapolation of correlation energies. The core-valence correction ΔE_{CV} is computed as the CCSD(T) energy difference between all electron and frozen-core calculations employing the cc-pCVTZ basis set.[64]

The diagonal Born−Oppenheimer correction ΔE_{DBOC}[46−49] and the scalar relativistic contribution to the energy ΔE_{rel}[50,51] are computed at the HF-SCF/aug-cc-pVDZ and CCSD(T)/aug-cc-pCVDZ levels, after having checked their convergence with respect to contributions calculated with triple-ζ basis sets for a few stationary points.

Finally, the corrections due to full treatment of triple (ΔE_{fT}) and perturbative treatment of quadruple (ΔE_{pQ}) excitations are computed, within the fc approximation, as energy differences between CCSDT and CCSD(T) and between CCSDT(Q) and CCSDT calculations employing the cc-pVTZ and cc-pVDZ basis sets, respectively.

Kinetic Models. Global and channel-specific rate constants were computed solving the multiwell one-dimensional master equation using the chemically significant eigenvalue (CSE) method within the Rice−Ramsperger−Kassel−Marcus (RRKM) approximation.[67] The collisional energy-transfer probability is described using the exponential down model[68] with a temperature-dependent ΔE_{down} of $260 \times (T/298)^{0.875}$ cm^{-1} in an argon bath gas.

For channels ruled by a distinct saddle point, rate coefficients are determined by the conventional transition-state theory (TST) within the rigid-rotor harmonic-oscillator (RRHO) approximation[69] and including tunneling as well as nonclassical reflection effects using the Eckart model.[70] Instead, rate constants for barrierless elementary reactions are computed employing the phase space theory (PST),[71,72] again within the RRHO approximation. The isotropic attractive potential V_{eff} entering the PST is described by a $\frac{C}{R^6}$ power law, whose C coefficient is obtained by fitting rev-DSD energies computed at various long-range distances of fragments. We obtained the following C coefficients for the PST calculations of barrierless channels: 230 $a_0^6 E_h$ for the $H_2S + Cl$ entrance channel, 64.2 $a_0^6 E_h$ for the $CH_3NH_2 + CN$ entrance channel on the methyl side, and 94.4 $a_0^6 E_h$ for the $CH_3NH_2 + CN$ entrance channel on the nitrogen side.

Table 2. Theoretical Values of Barrier Heights for the Forward and Reverse Reactions in the NHTBH38/08 Data Set Not Included in the DBH24 Selection[d]

	reaction		forward/reverse barrier height	
		jChS	jChS[a]	ref 38
NHT1	$H^\bullet + FH \rightarrow HF + H^\bullet$	41.99/41.99	42.02/42.02	42.18/42.18
NHT2	$H^\bullet + FCH_3 \rightarrow HF + CH_3^\bullet$	30.31/57.54	30.31/57.54	30.38/57.02
NHT3*	$H^\bullet + F_2 \rightarrow HF + F^\bullet$	3.50/107.18[b]	1.49/105.25	2.27/105.80
NHT4	$F^- + CH_3F \rightarrow FCH_3 + F^-$	−0.70/−0.70	−0.71/-0.71	−0.34/−0.34
NHT5	$F^-\cdots CH_3F \rightarrow FCH_3\cdots F^-$	13.21/13.21	13.20/13.20	13.38/13.38
NHT6	$Cl^- + CH_3Cl \rightarrow ClCH_3 + Cl^-$	2.27/2.27	2.33/2.33	3.10/3.10
NHT7	$F^- + CH_3Cl \rightarrow FCH_3 + Cl^-$	−12.32/19.29	−12.31/19.31	−12.54/20.11
NHT8	$OH^-\cdots CH_3F \rightarrow HOCH_3\cdots F^-$	11.14/47.38	11.14/47.38	10.96/47.20
NHT9	$H^\bullet + CO \rightarrow HCO^\bullet$	3.22/22.87	3.19/22.82	3.17/22.68
NHT10	$CH_3^\bullet + C_2H_4 \rightarrow CH_3CH_2CH_2^\bullet$	6.37/32.77	6.35/32.74	6.85/32.97
	MAX[c]	0.83	0.80	
	MUE[c]	0.33	0.32	
	RMSD[c]	0.42	0.40	

[a]jChS on QCISD/MG3 geometry. [b]Employing restricted open-shell geometry; the values using the unrestricted geometry are 4.46/108.14. [c]Neglecting the problematic reaction NHT3 (marked with an asterisk; see the text for discussion). [d]All of the values (exclusive of ZPE) are in kcal mol^{-1}.

The rate constants of the overall reactions evaluated in different temperature ranges are fitted by the three-parameter modified Arrhenius equation proposed by Kooij[73,74]

$$k(T) = A\left(\frac{T}{300}\right)^n \exp\left(-\frac{E}{RT}\right) \quad (6)$$

where A, n, and E are the fitting parameters and R is the universal gas constant.

RESULTS AND DISCUSSION

In the original jChS model, geometries and force fields were computed with the B2PLYP double-hybrid functional[75]
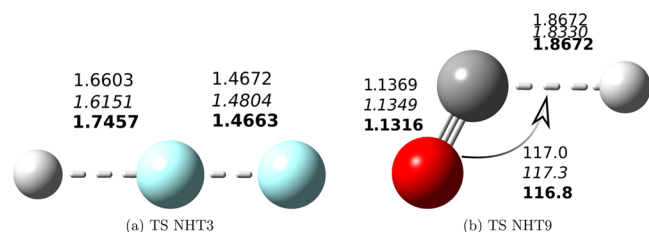
Figure 1. Sketch of the structures of the transition states ruling the reactions $H^\bullet + F_2 \rightarrow HF + F^\bullet$ (NHT3) and $H^\bullet + CO \rightarrow HCO^\bullet$ (NHT9). The key geometrical parameters issuing from rev-DSD, QCISD/MG3 (italics), and jChS (bold) geometry optimizations are also reported. Bond distances are in Å, and angles are in degrees. The following colors are used for the different atom types: white, H; black, C; red, O; and light blue, F.

augmented by empirical dispersion contributions (namely, the D3(BJ) model)[76,77] in conjunction with partially augmented triple-zeta basis sets.[33] However, the recently developed rev-DSD model[56] delivers improved descriptions of noncovalent interactions and activation energies.[78,79] Therefore, we benchmarked the performances of this functional (still in conjunction with partially augmented triple-zeta basis sets) for geometrical parameters and vibrational frequencies, obtaining results close to those delivered by the CCSD(T) ansatz in conjunction with comparable basis sets, but at a much reduced computational cost.[80] As a consequence, the jChS

model chemistry now uses by default rev-DSD geometries and force fields.

If the spin contamination from higher spin states is large, the potential energy surfaces computed by unrestricted wave functions can be significantly distorted, showing, for example, anomalously high reaction barriers.[81] This means that UMP2 estimates of CBS and CV contributions in the jChS model could become problematic. On the other hand, CCSD fully eliminates the $S + 1$ contaminant[82] and CCSD(T) reduces also the $S + 2$ contaminant[83] so that calculations at the CCSD(T) level are usually relatively insensitive to the choice of (restricted or unrestricted) orbitals.[84] However, in cases where higher spin contaminants become important, CCSD(T) can also fail.[83] On these grounds, all of the jChS and CBS-CVH energies have been computed by the restricted open-shell approach.

Concerning density-functional theory (DFT) methods, it is well-known that the extent of spin contamination in unrestricted versions of hybrid density functionals increases with the amount of HF exchange.[85] However, Menon and Radom[86] showed that in unrestricted double-hybrid procedures, the opposing behavior of UHF and UMP2 with respect to spin contamination leads to smaller differences between the energies predicted by unrestricted and restricted open-shell variants. Although rev-DSD energies are not used in the present context, spin contamination can have an effect also on gradients and Hessians. We have, therefore, checked systematically the spin contamination and found that its effect is always negligible (within the target accuracy of the jChS model) except for the CN radical and the transition state ruling the reaction $H^\bullet + F_2 \rightarrow HF + F^\bullet$, which will be analyzed in detail in a following section.

Reaction Barriers. The most well-known database of accurate reaction barriers is the DBH24 compilation[38,87] containing results mostly obtained at the CCSDTQ5/CBS level via the W4 theory[88] for a statistically representative set including three prototypes for each of the following classes of reactions: heavy-atom transfer, nucleophilic substitution, unimolecular and association reactions, and hydrogen-transfer reactions.

Table 3. Theoretical Values of Barrier Heights for the Forward and Reverse Reactions in the HTBH38/08 Data Set Not Included in the DBH24 Selection[e]

	reaction		forward/reverse barrier height		
		jChS	jChS[a]	ref 38	
HT1*[b]	$H^\bullet + HCl \rightarrow H_2 + Cl^\bullet$	4.97/7.80	5.57/7.95	5.49/7.42	
HT2[c]	$OH^\bullet + H_2 \rightarrow H_2O + H^\bullet$	5.67/21.76	5.58/21.69	5.10/21.20	
HT3	$CH3^\bullet + H_2 \rightarrow CH_4 + H^\bullet$	11.96/14.64	11.95/14.64	12.10/15.30	
HT4	$H^\bullet + H_2 \rightarrow H_2 + H^\bullet$	9.58/9.58	9.58/9.58	9.60/9.60	
HT5*[c]	$OH^\bullet + NH_3 \rightarrow H_2O + NH_2^\bullet$	4.13/14.41	3.55/13.85	3.20/12.70	
HT6[b]	$HCl + CH_3^\bullet \rightarrow Cl^\bullet + CH_4$	1.69/7.19	1.70/7.61	1.70/7.90	
HT7[c]	$OH^\bullet + C_2H_6 \rightarrow H_2O + C_2H_5^\bullet$	4.00/20.91	3.84/20.75	3.40/19.90	
HT8	$F^\bullet + H_2 \rightarrow HF + H^\bullet$	1.69/33.90	1.77/34.00	1.80/33.40	
HT9*[b,c]	$^3O + CH_4 \rightarrow OH^\bullet + CH_3^\bullet.$	14.77/9.83	14.87/9.82	13.70/8.10	
HT10*	$H^\bullet + PH_3 \rightarrow PH_2^\bullet + H_2$	2.85/25.09	2.82/25.05	3.10/23.20	
HT11*[b,c]	$^3O + HCl \rightarrow OH^\bullet + Cl^\bullet$	10.81/11.38	10.85/11.70	9.80/10.40	
HT12*	$NH_2^\bullet + CH_3^\bullet \rightarrow CH_4 + NH$	9.49/22.09	9.50/22.11	8.00/22.40	
HT13*	$NH_2^\bullet + C_2H_5 \rightarrow NH + C_2H_6$	9.97/19.08	10.39/19.51	7.50/18.30	
HT14	$NH_2^\bullet + C_2H_6 \rightarrow NH_3 + C_2H_5^\bullet$	11.24/17.85	11.18/17.80	10.40/17.40	
HT15	$NH_2^\bullet + CH_4 \rightarrow NH_3 + CH_3^\bullet$	13.82/16.94	13.80/16.92	14.50/17.80	
HT16*	$s-trans\ cis\text{-}C_5H_8 \rightarrow$ same	39.66/39.66	39.63/39.63	38.40/38.40	
	MAX[d]	1.01	0.88		
	MUE[d]	0.48	0.42		
	RMSD[d]	0.58	0.52		

[a]jChS on QCISD/MG3 geometry. [b]Spin−orbit corrections on the reverse reaction barrier. [c]Spin−orbit corrections on the forward reaction barrier. [d]Neglecting the problematic reactions (marked with an asterisk). [e]All of the values (exclusive of ZPE) are in kcal mol^{-1}.
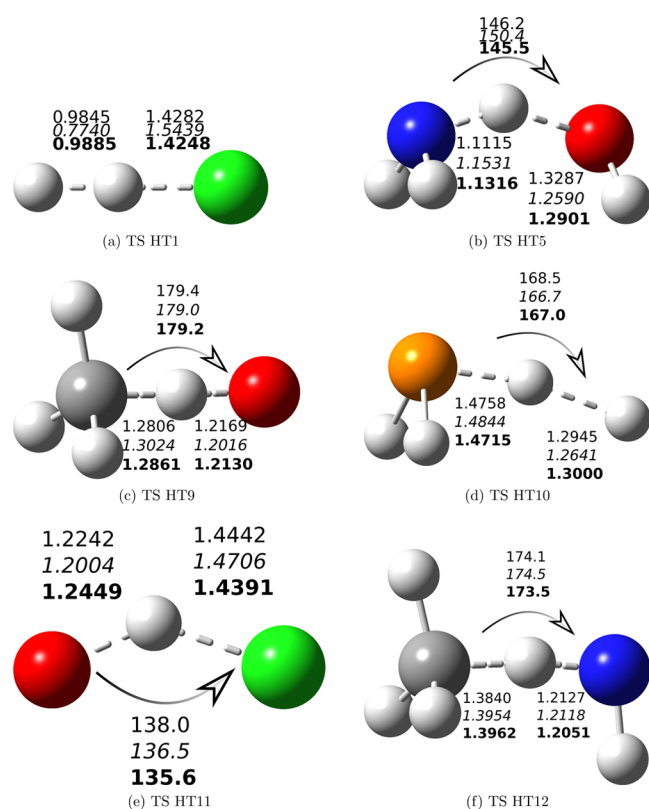

Figure 2. Sketch of the structures of the transition states ruling the reactions collected in Table 4. The key geometrical parameters issuing from rev-DSD, QCISD/MG3 (italics), and jChS (bold) geometry optimizations are also reported. Bond distances are in Å, and angles are in degrees. The following colors are used for the different atom types: white, H; black, C; blue, N; red, O; orange, P; and green, Cl.

Table 1 compares the reaction barriers computed at CCSD(T) and jChS levels to the reference values of ref 38. The arithmetic (mean unsigned error—MUE) and geometric (root-mean-square deviation—RMSD) average errors show that the jChS model chemistry fulfills the target of subchemical accuracy without any outlier above 1 kcal mol^{-1} (max error = 0.80 kcal mol^{-1}). It is also remarkable that estimation of CBS and CV contributions by inexpensive MP2 computations and without any empirical parameter halves the error of the underlying CCSD(T) computation. To investigate the role of geometries on the computed barriers, we repeated the computations using the QCISD/MG3 structures employed in the original compilation.[38] It is quite apparent that in this case the results are only marginally affected by geometry optimizations at different computational levels. We will come back to this aspect in the following since the situation could be different for more complex transition structures and/or the noncovalent complexes ruling the entrance channels of barrierless reactions. In this connection, further support to the reliability of rev-DSD structures is provided by the respectable MUE and RMSD (1.7 and 2.4 kcal mol^{-1}, respectively) of the energy barriers computed at this level.

Zhang and co-workers[18] have shown that, for the same set of reactions, inclusion of explicit correlation (F12) in CCSD(T) computations[89] reduces the mean and maximum unsigned errors of the conventional CCSD(T) approach (0.66 and 1.77 kcal mol^{-1}) to 0.29 and 0.85 kcal mol^{-1} when using basis sets slightly larger than j3Z (including also f diffuse functions on non-hydrogen atoms). As shown in Table 1, this improvement is close to that obtained when going from CCSD(T)/j3Z (0.71 and 2.49 kcal mol^{-1}) to jChS (0.36 and 0.80 kcal mol^{-1}). These trends suggest that inclusion of explicit correlation or two-point extrapolation at the MP2 level is an effective route for improving significantly the accuracy of computed energy barriers, without introducing additional computational bottlenecks with respect to the underlying CCSD(T)/j3Z reference.

Table 4. Theoretical Values of the Forward and Reverse Barriers Ruling the "Challenging" HTBH38/08 Reactions[d]

geometry		QCISD		rev-DSD	jChS		
	forward/reverse barrier	ref 38	jChS[a]	jChS	jChS	CBS-CV	CBS-CVH
HT1[a]	$H^{\bullet} + HCl \rightarrow H_2 + Cl^{\bullet}$	5.49/7.42	5.57/7.95	4.97/7.80	4.97/7.85	5.25/8.23	5.41/8.19
HT5[b]	$OH^{\bullet} + NH_3 \rightarrow H_2O + NH_2^{\bullet}$	3.20/12.70	3.55/13.85	4.13/14.41	4.41/14.60	4.40/14.34	4.39/13.63
HT9[a,b]	$^3O + CH_4 \rightarrow OH^{\bullet} + CH_3^{\bullet}$	13.70/8.10	14.87/9.82	14.77/9.83	14.93/9.76	14.70/9.37	14.64/9.30
HT10	$H^{\bullet} + PH_3 \rightarrow PH_2^{\bullet} + H_2$	3.10/23.20	2.82/25.05	2.85/25.09	2.85/25.12	2.87/24.48	2.89/24.52
HT11	$^3O + HCl \rightarrow OH^{\bullet} + Cl^{\bullet}$	9.80/10.40	10.85/11.70	10.81/11.38	10.67/11.43	10.93/11.34	10.27/10.98
HT12	$NH_2^{\bullet} + CH_3^{\bullet} \rightarrow CH_4 + NH$	8.00/22.40	9.50/22.11	9.49/22.09	8.94/21.84	8.87/21.89	9.24/22.26
	MAX[c]	1.32	0.84	0.57	0.60	0.66	
	MUE[c]	0.74	0.39	0.34	0.34	0.20	
	RMSD[c]	0.87	0.46	0.38	0.38	0.28	

[a]Spin−orbit corrections on the reverse reaction barrier. [b]Spin−orbit corrections on the forward reaction barrier. [c]Neglecting the reverse barrier of reaction HT5. [d]All of the values (exclusive of ZPE) are in kcal mol^{-1}.

(a) b1 BHPERI1   (b) b2 CRBH1   (c) b3 CRBH4

(d) b4 CADBH1   (e) b5 CADBH4   (f) b6 PXBH1
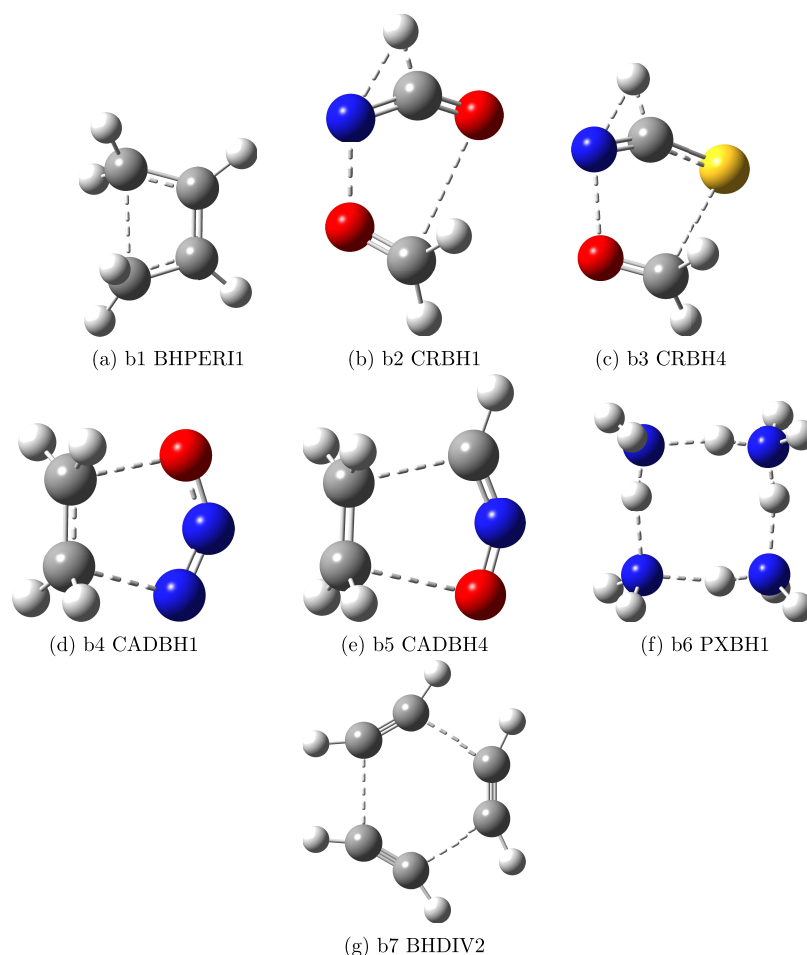
(g) b7 BHDIV2

Figure 3. Sketch of the structures of the transition states ruling the reactions of Table 5. The following colors are used for the different atom types: white, H; black, C; blue, N; red, O; and yellow, S.

As a matter of fact, already for reactions involving two heavy atoms (e.g., A7, A8, A9, A10 in Table 1), single-point jChS computations require no more than twice the time of the CCSD(T)/jun-cc-pVTZ step and are an order of magnitude faster than the CBS-CV counterparts. On increasing the dimensions of the systems, the effectiveness of the jChS model increases because of the favorable scaling of MP2 computations with respect to CCSD(T) ones, which can be further enhanced by approaches employing resolution of identity and other acceleration techniques. Furthermore, jChS computations can be performed also with the widely diffused electronic

structure codes lacking explicitly correlated approaches (e.g., Gaussian or CFOUR), and the accuracy of the results surpasses that of all of the model chemistries considered by Zheng et al.[38]

Two larger databases of prototypical reactions are also available for barriers related to transfers of hydrogen and non-hydrogen atoms (HTBH38[39] and NHTBH38,[40] respectively). However, the reaction barriers not already included in the DBH24 set have been obtained at a lower computational level (W1). We have thus decided to compute at the jChS level all of the reactions of the above two sets not contained in the

Table 5. Theoretical Values of Barrier Heights for the Forward and Reverse Reactions in the BH14 Data Set, Obtained at Different Levels of Theory[h]

	label in BH28	forward/reverse barrier height	forward reaction barrier height		
		jChS	jChS[a]	W3lite-F12[b]	CCSDT(Q)-CCSD(T)
b1	BHPERI1[c]	35.07/95.13		35.01	−0.17
b2	CRBH1[d]	47.24 (78.59)	47.01	46.15	−1.10
b3	CRBH4[d]	46.54 (64.14)	46.12	44.89	−1.60
b4	CADBH1[e]	27.26/36.08		27.56	0.00
b5	CADBH4[e]	11.57/57.52		11.64	−0.24
b6	PXBH1[f]	48.59/48.59		48.45	−0.12
b7	BHDIV2[g]	51.15/201.05		50.10	−0.14
	MAX	1.65			
	MUE	0.62			
	RMSD	0.86			

[a]Using the geometries of ref 41. [b]Ref 41. [c]Refs 90, 91. [d]Ref 92. [e]Refs 91, 93. [f]Ref 94. [g]Ref 95. [h]All of the values (exclusive of ZPE) are in kcal mol^{-1}.

Table 6. ThCS21 Database: ZPEs in kcal mol^{-1} and Absolute Entropies at 298.15 K and 1 atm in cal (mol K)$^{-1}$

molecule	ZPE$_{harm}$[a]	ZPE$_{anh}$[a,b]	ZPE$_{exp}$[c]	S$_{harm}$[a]	S$_{exp}$[d]
HF	5.89	5.84	5.86	41.46	41.50
HCl	4.30	4.27	4.24	44.57	44.64
H$_2$	6.36 (6.24)	6.30	6.23	31.13	31.20
N$_2$	3.33	3.32	3.36	45.77	45.77
F$_2$	1.42	1.41	1.30	48.33	48.44
CO	3.09	3.08	3.09	47.24	47.21
Cl$_2$	0.81	0.81	0.80	53.18	53.29
CO$_2$	7.26	7.23	7.30	51.09	51.07
CS$_2$	4.36	4.35	4.34	56.78	56.85
H$_2$O	13.45 (13.21)	13.24	13.26	45.09	45.10
H$_2$S	9.59	9.47	9.48	49.12	49.16
HOF	8.77 (8.65)	8.64	8.65	54.11	54.17
HOCl	8.31 (8.19)	8.19	8.19	56.47	56.49
N$_2$O	6.84	6.80	6.77	52.51	52.54
HCN	10.03 (9.91)	9.95	10.00	48.16	48.21
SO$_2$	4.33	4.31	4.41	59.35	59.30
C$_2$H$_2$	16.72 (16.48)	16.56	16.49	47.91	47.99
H$_2$CO	16.76 (16.52)	16.54	16.52[e]	52.23	52.30
NH$_3$	21.63 (21.27)	21.26	21.20	45.98	46.04
CH$_4$	28.20 (27.72)	27.79	27.71	44.48	44.48
C$_2$H$_4$	32.06 (31.58)	31.67	31.46[f]	52.35	52.39
MUE	0.15 (0.04)	0.05		0.05	
RMSD	0.22 (0.06)	0.07		0.06	

[a]rev-DSD-PBEP86-D3(BJ)/jun-cc-pV(T + d)Z. [b]HDCPT2 model. [c]From ref 96. [d]From ref 104. The original values have been lowered by 0.03 cal (mol K)$^{-1}$ to take into account the passage from 1 bar (0.1 MPa) to 1 atm (0.10135 MPa) references. [e]From accurate diffusion Monte Carlo computations[105] since the value of 16.10 reported in ref 96 is affected by an estimated error of 0.51 kcal mol^{-1}. [f]From the accurate computations of ref 106 since the value of 30.70 reported in ref 96 is affected by an estimated error of 0.40 kcal mol^{-1}.

original DBH24 compilation using both rev-DSD and the original QCISD/MG3 geometries. Whenever significant discrepancies were found, the reactions were recomputed also at the CBS-CVH level.

The reactions from the NHTBH38 set not included in the DBH24 selection are collected in Table 2. It is noteworthy that

Table 7. Absolute Entropies at 298.15 K and 1 atm in cal (mol K)$^{-1}$

molecule	S$_{harm}$[a]	S$_{HR}$[a,b]	S$_{exp}$
CH$_3$CH$_3$	54.38	54.70	54.79[c,d]
CH$_3$OH	57.00	57.36	57.29[c,d]
CH$_3$SH	60.57	60.99	60.96[c,d]
CH$_3$CHO	62.66	63.11	63.06[c,d]
CHOCHO	64.93	65.09	65.10[c,e]

[a]rev-DSD-PBEP86-D3(BJ)/jun-cc-pV(T+d)Z. [b]Including HR correction. [c]The original values have been lowered by 0.03 cal (mol K)$^{-1}$ to take into account the passage from 1 bar (0.1 MPa) to 1 atm (0.10135 MPa) references. [d]From ref 111. [e]From ref 112.

rev-DSD energy barriers, although not directly used in the jChS model chemistry, show MUEs smaller than 2.0 kcal mol^{-1}, thus suggesting that the corresponding geometries should be sufficiently accurate for single-point energy evaluations at higher computational levels. This is confirmed by the finding that only for reaction NHT3, QCISD and rev-DSD geometries lead to significantly different results (cf. columns 2 and 3 of Table 2). Geometry optimization at the jChS level provides results far from both values (Figure 1a). However, as mentioned in a previous section, unrestricted rev-DSD computations show a strong spin contamination for the TS ruling reaction NHT3 ($\langle S^2 \rangle$ = 1.03 in place of the correct value of 0.75). We have, therefore, reoptimized the geometry of this TS employing the restricted open-shell approach in conjunction with numerical energy derivatives. The issuing geometrical parameters (rHF = 1.6603, rFF = 1.4672 Å) are closer to the jChS counterparts (rHF = 1.7457, rFF = 1.4663 Å) than the unrestricted values (rHF = 1.5700, rFF = 1.4021 Å) and, indeed, even better than the QCISD/MG3 values of ref 38 (rHF = 1.6151, rFF = 1.4804 Å), thus giving further support to the accuracy of rev-DSD geometries. To check the accuracy of computed energies irrespective of geometry effects, we have recomputed the forward and reverse barriers of reaction NHT3 at the CBS-CVH level employing QCISD/MG3 geometries. The results (1.57 and 104.84 kcal mol^{-1}) are much closer to the jChS values (1.49 and 105.25, MUE = 0.25 kcal mol^{-1}) than to the results of ref 38 (2.27 and 105.80, MUE = 0.83 kcal mol^{-1}), thus confirming the reliability and robustness of the jChS model chemistry. However, in this case, fully reliable results can be obtained only employing more accurate geometries: as a matter of fact, the forward and reverse barriers obtained from single-point CBS-CVH computations at jChS geometries are 2.59 and 105.77 kcal mol^{-1}, respectively. The seemingly good agreement with the results of ref 38 is due to a fortuitous error compensation between poor geometry and limited accuracy of the electronic energy. With the exception of this reaction, the agreement between jChS energies and the reference values is satisfactory, suggesting that for this kind of reaction the jChS errors are in line with those discussed above for the DBH24 database.

The reactions from the HTBH38 set not included in the DBH24 selection are collected in Table 3. Once again, it is noteworthy that the rev-DSD energy barriers, although not directly used in the jChS model chemistry, do not show any unrealistic outlier. Only for reactions HT1 and HT5, QCISD and rev-DSD geometries lead to significantly different results (cf. columns 2 and 3 of Table 3). Geometry optimization at the jChS level provides results close to rev-DSD (Figure 2a) for HT1 and intermediate between rev-DSD and QCISD for

Table 8. ThOS10 Database: ZPEs and Nonpotential Energy Terms for Representative Open-Shell Species at 298.15 K and 1 atm in cal (mol K)$^{-1}$

molecule	$ZPE_{calc}^{a,b}$	ZPE_{exp}^{b}	$S_{calc}^{a,c}$	$S_{exp}^{c,d}$	$H-H_{calc}^{0\ a,b}$	$H-H_{exp}^{0\ b,e}$
OH($^2\pi$)	5.25 (5.33)	5.29[e]	43.95	43.88	2.07	2.11
SH($^2\pi$)	3.88 (3.88)	3.82	47.27	46.76	2.07	2.07
CN($^2\sum^{+,f}$)	2.83 (2.83)	2.95	48.35	48.43	2.07	2.07
NO($^2\pi$)	2.80 (2.77)	2.71	50.42	50.34	2.07	2.07
NH$_2$($^2B_1$)	11.89 (11.83)	11.52[g]	46.49	46.54	2.37	2.37
HCO(^{2}A')	8.06 (8.09)	8.09[h]	53.58	53.66	2.39	2.39[h]
HO$_2$(^{2}A'')	8.85 (8.87)	8.78[i]	54.67	54.76	2.39	2.39
CH$_3$(^{2}A$_2$'')	18.62 (18.42)	18.48[i]	46.26	46.38	2.46	2.45
t-HOCO(^{2}A')	13.00 (13.07)	13.10[i]	60.08		2.61	
CH$_3$CO(^{2}A')	26.82 (26.85)	26.69[i]	64.23	63.92	2.98	2.96

[a]rev-DSD-PBEP86-D3(BJ)/jun-cc-pV(T + d)Z HRHO model and (in parenthesis) HRHO model including a correction to ZPEs of −0.12 for each CH, NH, or OH bond. [b]In kcal mol^{-1}. [c]In cal (mol K) $^{-1}$. [d]From ref 113. When needed, entropy values have been lowered by 0.03 cal (mol K)$^{-1}$ to take into account the passage from 1 bar (0.1 MPa) to 1 atm (0.10135 MPa) references. [e]From ref 96. [f]Restricted open shell with an equilibrium bond length of 1.179 Å;; the unrestricted result is 3.43 kcal mol^{-1} with S^2 = 0.854 and an equilibrium bond length of 1.159 Å. [g]CBS-CV results from ref 114. [h]CBS-CV results from ref 115. [i]Diffusion Monte Carlo results from ref 105.

$$H^{\bullet} + CO \longrightarrow HCO^{\bullet}$$
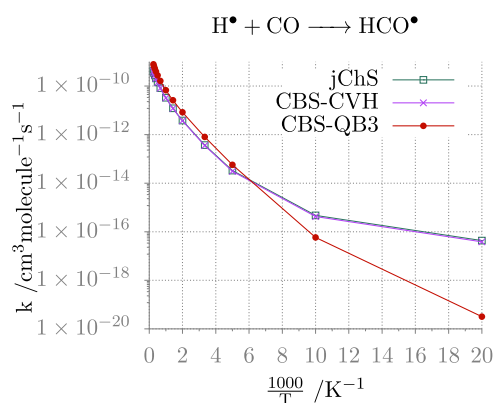
Figure 4. Temperature dependence of the H$^{\bullet}$ + CO reaction rate constants calculated at various levels of theory in the high-pressure limit.

HT5 (Figure 2b). The agreement between jChS energies and the reference values is generally worse than for the NHTBH38 set and particularly disappointing for reactions HT1, HT5, HT9, HT10, HT11, HT12, HT13, and HT16. To have a first check of the accuracy of the jChS results irrespective of geometry effects, the forward and reverse barriers of two reactions in this group (HT1 and HT12) have been recomputed at the CBS-CVH level on top of QCISD/MG3 geometries. In the first case, the CBS-CVH values (5.95 and 8.73 kcal mol^{-1}) are quite close to the results of both ref 38 and the jChS counterparts for the forward barrier and much closer to the jChS result for the reverse barrier. The situation is reversed for reaction HT12, where the CBS-CVH results (9.35 and 22.37 kcal mol^{-1}) confirm the similar results of jChS and ref 38 for the reverse barrier but are much closer to the jChS ones for the forward barrier. Once again, the jChS model chemistry does not show any outlier above the threshold of

chemical accuracy, whereas this is not the case for the original reference values of ref 38. For the forward and reverse barriers of the remaining eight reactions, the deviations of the jChS results from those of ref 38 are well within subchemical accuracy (MUE around 0.5 kcal mol^{-1}).

We then selected six "challenging reactions" among those mentioned above for further investigation. To this end, we report in Table 4 the results obtained at different geometries together with new reference values obtained at the CBS-CVH level on top of jChS geometries. A first general remark is that some of the new reference values differ by more than 1 kcal mol^{-1} from those reported in ref 38 (cf. columns 1 and 6 of Table 4). Furthermore, the only barrier showing significant contributions by higher-order terms (mainly full triple and perturbative quadruple excitations) is the reverse barrier of reaction HT5 (cf. columns 5 and 6 in Table 4). Neglecting this barrier, the results of ref 38 show an MUE of 0.82 kcal mol^{-1} and a maximum error of 1.61 kcal mol^{-1}, whereas the jChS approach has an MUE lower than 0.40 kcal mol^{-1} without any absolute error larger than 1 kcal mol^{-1}, irrespective of the level of geometry optimizations. As a matter of fact, the relatively cheap rev-DSD geometries can be confidently employed for reaching subchemical accuracy and the use of more accurate structures does not really improve the results. The CBS-CV approach reduces significantly the MUE, but at the price of employing more accurate (and costly) geometries together with CCSD(T) computations performed with partially augmented 4Z basis sets. In conclusion, the jChS model chemistry can be confidently employed for evaluating reaction barriers of all of the reactions included in the HTBH38 and NHTBH38 data sets with subchemical accuracy without any outlier above 1 kcal mol^{-1}.

To extend the benchmark to larger and more complex systems, we resorted to the BH28 set of ref 41, which includes accurate (W3lite-F12) energy barriers for several pericyclic

Table 9. Arrhenius−Kooij Parameters for the H$^{\bullet}$ + CO Reaction

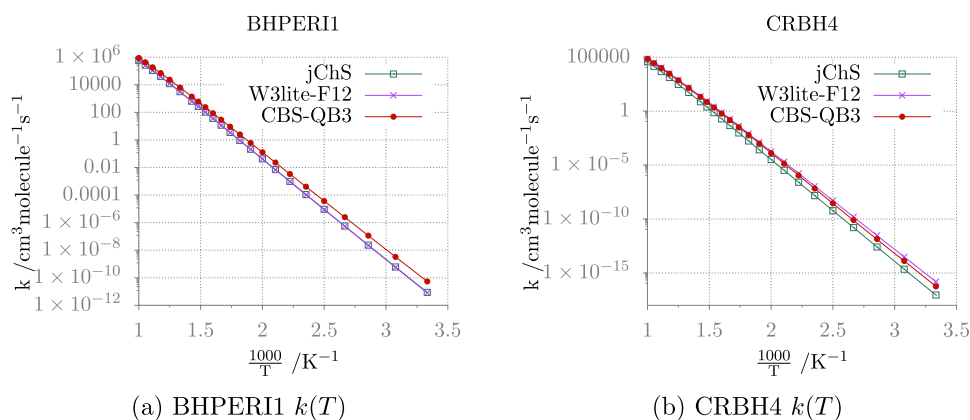| forward/reverse	ref 116	jChS	CBS-CVH	CBS-QB3
A (cm^3 molecule^{-1} s^{-1})	2.98×10^{-11}/1.37×10^{13}	3.86×10^{-11}/1.47×10^{13}	3.87×10^{-11}/1.46×10^{13}	7.96×10^{-11}/ 3.81×10^{13}
n	1.03/1.06	1.07/1.20	1.06/1.20	1.02/1.04
E (kcal mol^{-1})	2.64/17.79	2.86/18.14	2.89/18.08	2.76/17.95
rms		4×10^{-14}/ 3.20×10^{-2}	3.9×10^{-14}/3.21×10^{-2}	1.91×10^{-14}/ 2.56×10^{-2}

(a) BHPERI1 $k(T)$　　　　　　　(b) CRBH4 $k(T)$

Figure 5. Rate constant temperature-dependence plots of the BHPERI1 and CRBH4 reactions from the BH14 data set for a pressure of 1 atm.

Table 10. Arrhenius−Kooij Parameters for BHPERI1 and CRBH4 Reactions from the BH14 Data Set

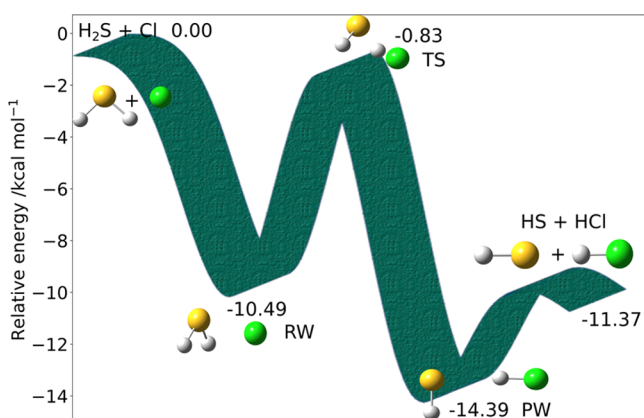|	BHPERI1			CRBH4		
	jChS	W3lite-F12	CBS-QB3	jChS	W3lite-F12	CBS-QB3
A (cm^3 molecule^{-1} s^{-1})	7.43×10^{13}	8.18×10^{13}	1.26×10^{14}	1.24×10^{16}	2.58×10^{16}	1.14×10^{17}
n	-1.05	-1.12	-1.44	-2.81	-3.37	-4.02
E (kcal mol^{-1})	34.31	34.41	33.53	45.60	44.35	45.83
rms	7.67×10^{-2}	7.80×10^{-2}	1.06×10^{-1}	1.05×10^{-1}	1.08×10^{-1}	1.06×10^{-1}

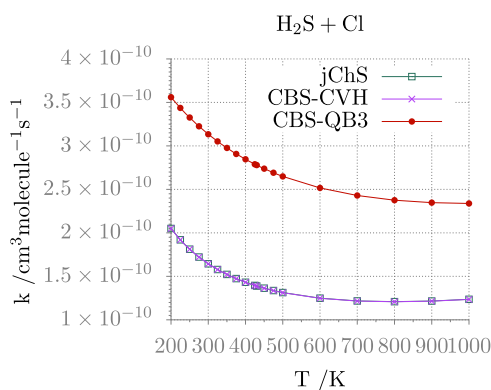**Figure 6.** H_2S + Cl reaction mechanism. Electronic energies are computed at the jChS level.

Figure 7. Temperature-dependence plots of the H_2S + Cl reaction rate constants calculated at various levels of theory for a pressure of 1 atm.

(BHPERI), bipolar cycloaddition (CADBH), cycloreversion (CRBH), multiple proton exchange (PXBH), and different

(BHDIV) reactions. For each of these five classes of reactions, we selected no more than two representative cases. The structures of the seven selected transition states are shown in Figure 3, and the corresponding forward and reverse reaction barriers (BH14 set) are collected in Table 5.

The average and maximum errors are larger than those of the DBH24 set; however, a closer inspection of the results shows that, as already pointed out in ref 41, the role of full triple and quadruple excitations is non-negligible for CRBH reactions. This effect cannot be captured, of course, by the jChS model and leads to errors well above 1 kcal mol^{-1}. In all other cases, the errors are below the target of the jChS model chemistry. As a matter of fact, excluding the contribution of triple and quadruple excitations (last column in Table 5) reduces the MUE of jChS results to 0.24 kcal mol^{-1}. Furthermore, the error related to the difference between rev-DSD and reference geometries is lower than 0.3 kcal mol^{-1} even in the worst cases.

Zero Point Energy and Finite Temperature Contributions. Accurate determination of thermochemical and kinetic parameters by quantum chemical methods requires, in addition to electronic energies, also zero point and finite temperature contributions (FTCs), which are usually obtained within the RRHO approximation, possibly employing empirical scaling factors.[96] However, it is well-known that the scaling factors are intrinsically different for zero point energies (ZPEs) and vibrational frequencies, with the results for the latter quantities often being not sufficiently accurate.[97] One effective strategy devoid of any empirical parameter is offered by the generalized second-order vibrational perturbation theory in conjunction with a separate treatment of large-amplitude motions.[58,98] In fact, a resonance-free expression for ZPEs of energy minima and transition states,[99,100] an unsupervised smoothing procedure (HDCPT2) for fundamental frequencies,[101] and a fully automatic detection and treatment of torsional motions (hindered rotor, HR, approximation)[102] have been implemented in the Gaussian code[60] and

Table 11. Arrhenius–Kooij Parameters for the H$_2$S + Cl Reaction

	jChS	CBS-CVH	CBS-QB3
A (cm^3 molecule^{-1} s^{-1})	9.12×10^{-11}	9.11×10^{-11}	2.63×10^{-10}
n	7.65×10^{-2}	7.67×10^{-2}	1.60×10^{-1}
E (kcal mol^{-1})	-3.42×10^{-1}	-3.42×10^{-1}	-9.94×10^{-2}
rms	2.51×10^{-12}	2.51×10^{-12}	2.87×10^{-12}
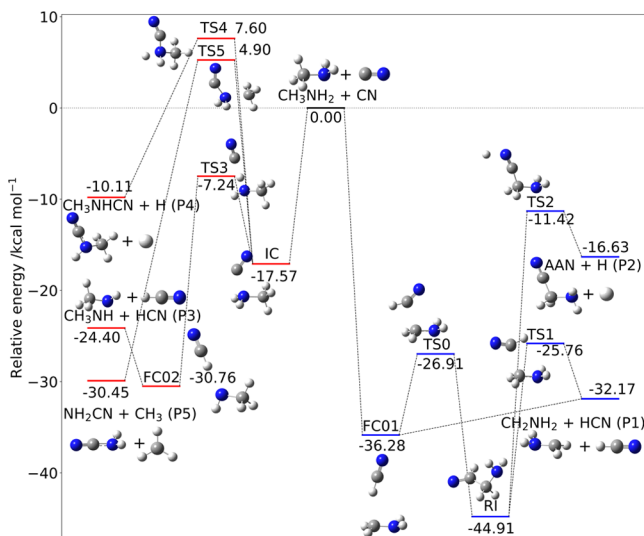
Figure 8. CH$_3$NH$_2$ + CN reaction mechanism. The pathway for the attack of CN to the N moiety of methylamine is marked in red and for the abstraction of H from the methyl group by CN in blue. Electronic energies are computed at the jChS level.

validated.[59] As a consequence, a fully black-box procedure is available for taking into account all of these contributions.

Next, the so-called simple perturbation theory (SPT)[103] can be applied for computing partition functions without the need for performing explicit (or stochastic) summations of individual energy levels. In fact, the SPT retains the formal expression of the harmonic partition function but employing the anharmonic ZPE and fundamental levels (Δ_i) issuing from HDCPT2 and HR computations.

$$Q_{vib} = \frac{\exp\left(-\frac{ZPE}{KT}\right)}{\prod_i \left[1 - \exp\left(-\frac{\Delta_i}{KT}\right)\right]} \qquad (7)$$

This approximation provides results in remarkable agreement with accurate reference values and leads to analytical expressions for the different thermodynamic functions.[103]

On these grounds, we will now analyze the performances of the jChS model chemistry in dealing with these terms starting from a benchmark of the RRHO approximation with reference to accurate quantum chemical results and then proceeding to take into account anharmonic contributions. For illustration purposes, we will focus our attention on ZPEs and absolute entropies (S), which are especially sensitive to high and low frequencies, respectively.

To this end, a new database has been built (ThCS21), which contains accurate experimental values for the ZPEs and absolute entropies of 21 semirigid closed-shell molecules, whose estimated errors are below 0.1 kcal mol^{-1} and 0.05 cal (mol K)$^{-1}$, respectively. The results collected in Table 6 show that already at the harmonic level, the errors are well within the level of accuracy expected from the jChS model chemistry and
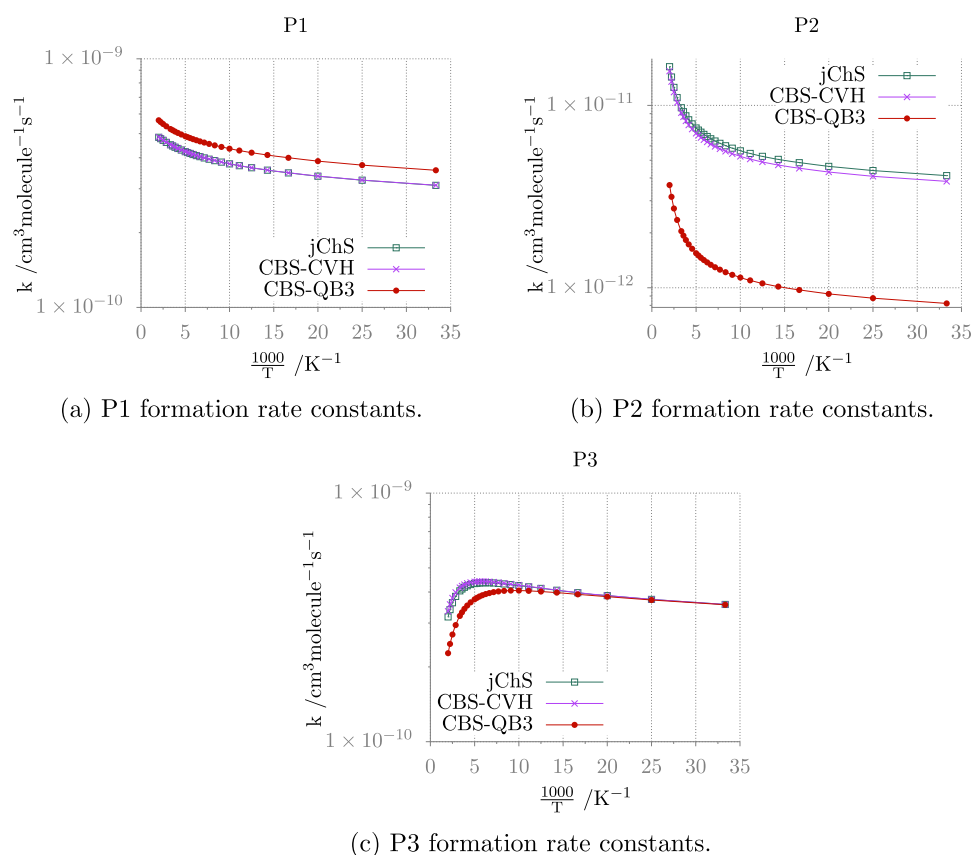
the anharmonic results can be confidently used in conjunction with the most sophisticated models (e.g., CBS-CVH). Actually, the harmonic frequencies obtained at this level do not require any empirical correction to compensate for method and/or basis set deficiency but only for genuine anharmonic effects, which, in turn, give significant contributions to ZPEs only for some XH bonds (X = C, N, O). As a consequence, an empirical correction of 0.12 kcal mol^{-1} for each bond of this kind provides results very close to the anharmonic counterparts (see results in parenthesis in the first column of Table 6).

Accurate entropy values are also available for the same set of molecules, and harmonic computations perform a remarkable job in reproducing the experimental values. However, entropy is exquisitely sensitive to low-frequency vibrations, so that a set of flexible molecules is collected in Table 7. It is apparent that the HRHO model (which does not add any computational burden with respect to the underlying RRHO model) performs a remarkable job for systems containing a single torsion. The situation is more involved for larger flexible systems due to the presence of several low-energy minima contributing to the overall thermodynamic functions. Although this aspect goes beyond the main topic of the present contribution, we point out that several strategies are being proposed, following systematic search,[107] stochastic,[108] and, more recently, machine learning[109] approaches. Other kinds of large-amplitude motions can be taken into account by means of one-dimensional variational or quasi-variational approaches[110] followed by SPT or direct count of energy levels.[98]

Another issue is represented by open-shell species, which are of paramount importance in both astrochemistry and atmospheric chemistry. In this case, experimental zero point energies are available only for diatomic species and accurate determinations are quite limited also for the other thermodynamic functions. The jChS results collected in Table 8 for a few representative systems (ThOS10 database) suggest that (in the absence of strong multireference effects) the expected accuracy is close to that reached for closed-shell systems.

Reaction Rates. In this section, we analyze the impact on reaction rates of the different ingredients discussed in the previous section, comparing the results issuing from different model chemistries including CBS-QB3, jChS, and CBS-CVH. Starting from simple elementary mechanisms, we proceed to more complex potential energy surfaces including several intermediates and transition states, possibly leading to different products.

The first test case is the high-pressure limit of the reaction H$^\bullet$ + CO, which has been recently investigated by Vichietti et al.[116] This reaction belongs to the HTBH38 set, whose jChS results have been discussed in the section devoted to energy barriers. For purposes of comparison, we have computed also the barriers at the CBS-CVH level on top of jChS geometries obtaining values (3.26 and 22.86 kcal mol^{-1}) for the forward and reverse barriers very close to the jChS counterparts at rev-DSD geometries (3.22 and 22.87 kcal mol^{-1}). Although the presence of a van der Waals prereactive complex has been

(a) P1 formation rate constants.

(b) P2 formation rate constants.

(c) P3 formation rate constants.

Figure 9. Temperature-dependence plots of the CH_3NH_2 + CN reaction rate constants calculated at various levels of theory for a pressure of 10^{-8} atm.

suggested, its stability (if any) is so small that its impact on the computed reaction rates is negligible.

The reaction rates computed in the 50−4000 K temperature interval are shown in Figure 4, and the parameters of the corresponding Arrhenius−Kooij fits obtained by different electronic structure methods are collected in Table 9. The non-Arrhenius behavior of the reaction is quite apparent, but the small errors of all of the fits show that the Arrhenius−Kooij model captures the essence of the deviation. Furthermore, the jChS results are close to the reference values of ref 116, whereas this is not the case for the largely employed CBS-QB3 approach at least at low temperatures.

We next consider the BHPERI1 and CRBH4 reactions discussed in the section on the energy barriers (see Figure 3a,c). The rates computed in the 300−1000 K temperature interval by different electronic structure methods are shown in Figure 5a,b, whereas the parameters of the corresponding Arrhenius−Kooij fits are collected in Table 10. Both reactions are characterized by quite high energy barriers, and their rates show a clear Arrhenius behavior. In these circumstances, the different electronic structure methods deliver comparable results over the whole temperature range.

The next example is the reactive potential energy surface for H_2S + Cl (see Figure 6), which involves a van der Waals prereactive complex (RW) followed by the transition state TS leading to a productlike van der Waals complex (PW) and then to the products, i.e., HS + HCl. Since this reaction has been recently investigated at the CBS-CVH level,[28] it represents a meaningful test for the jChS model chemistry. Once again, the largest deviation from the reference values for all of the

stationary points is lower than 0.3 kcal mol^{-1}, to be compared to errors larger than 1 kcal mol^{-1} especially for transition states at the CBS-QB3 level. Errors of this magnitude can lead to unreliable rate constants, especially for reactions like this where the dynamical bottleneck is located at the inner transition state, as already pointed out in ref 28.

The reaction rates issuing from jChS computations are compared in Figure 7 to the CBS-QB3 and CBS-CVH counterparts, whereas the parameters of the corresponding Arrhenius−Kooij fittings (see eq 6) are collected in Table 11. The root-mean-square deviations reported in Table 11 demonstrate that the data are indeed well fitted by the Arrhenius−Kooij expression with a negative activation energy (E) at 0 K. The results issuing from jChS and CBS-CVH computations are virtually indistinguishable, whereas significantly larger rates are obtained at the CBS-QB3 level.

The last example is the quite complex reactive potential energy surface ruling the addition of CN to CH_3NH_2 shown in Figure 8 together with the jChS energies of all of the stationary points. The experimental reaction rate at different temperatures[117] has been recently well reproduced employing CBS-CVH electronic structure computations within a master equation treatment similar to that employed in the present paper.[118] This system represents, therefore, a challenging test for the jChS model.

The attack of CN on the nitrogen side of methylamine proceeds via a potential well associated with a prereactive complex, $NC \cdots NH_2CH_3$ (IC), which evolves in an inner (submerged) transition state (TS3) that, passing through an $NCH \cdots NHCH_3$ intermediate (FC02), forms the HCN +

Table 12. Arrhenius–Kooij Parameters for the CH$_3$NH$_2$ + CN Reaction

	jChS			CBS-CVH			CBS-QB3		
	P1	P2	P3	P1	P2	P3	P1	P2	P3
A (cm^3 molecule^{-1} s^{-1})	4.51×10^{-10}	8.95×10^{-12}	4.28×10^{-10}	4.52×10^{-10}	8.38×10^{-12}	4.38×10^{-10}	5.22×10^{-10}	1.86×10^{-12}	3.54×10^{-10}
n	1.50×10^{-1}	8.70×10^{-1}	-2.43×10^{-1}	1.51×10^{-1}	8.84×10^{-1}	-2.09×10^{-1}	1.63×10^{-1}	9.78×10^{-1}	-4.45×10^{-1}
E (kcal mol^{-1})	2.10×10^{-3}	-8.31×10^{-2}	4.99×10^{-2}	2.02×10^{-3}	-8.48×10^{-2}	4.63×10^{-2}	5.28×10^{-4}	-9.72×10^{-2}	6.71×10^{-2}
rms	9.70×10^{-13}	4.54×10^{-13}	1.75×10^{-11}	9.40×10^{-13}	4.33×10^{-13}	1.69×10^{-11}	3.31×10^{-13}	1.11×10^{-13}	1.73×10^{-11}

NHCH$_3$ products (P3). Alternative channels, and in particular that leading to NH$_2$CN + CH$_3$, are ruled by nonsubmerged transition states and are, therefore, closed under the ISM conditions. The attack on the methyl side forms directly the FC01 complex, which, in turn, leads to HCN + NH$_2$CH$_2$ (P1) without any potential energy barrier. In this case, the alternative two-step mechanism (TS0-RI-TS2-P2) leading to aminoacetonitrile + H is open since it involves only submerged transition states, but it is less favorable.

Comparison with the CBS-CVH results of ref 118 shows MAE of 0.26 kcal mol^{-1} and a maximum deviation of -0.55 kcal mol^{-1} for the relative energies of all of the stationary points. The errors of the CBS-QB3[22] model are again larger than 1 kcal mol^{-1}, in agreement with the estimates of previous studies.[119] The reaction rates issuing from jChS computations are compared in Figure 9 with the CBS-QB3 and CBS-CVH counterparts, whereas the parameters of the corresponding Arrhenius–Kooij fits (see eq 6) are collected in Table 12. It is to be noted that pressure does not influence the reaction rate, as the reactants always proceed to form the products without experiencing significant collisional stabilization in the investigated pressure range (0.001–1 bar).

A curved Arrhenius plot is obtained when the activation energy depends on the temperature, and this behavior is captured by the Arrhenius–Kooij equation when this dependence is linear. The root-mean-square deviations reported in Table 12 demonstrate that the data for the different products are indeed well fitted by the Arrhenius–Kooij expression. Within this model, E represents the activation energy at 0 K, and the activation energy at a generic temperature T is given by $E + n\left(\frac{RT}{300}\right)$. In the present case, the activation energy is positive for P1 and P3 as a result of both the capture rate constant and the subsequent energy barriers for the unimolecular steps. The value is instead negative for P2, but in this case, the Arrhenius plot is essentially linear. The n parameter (the first derivative of the activation energy with respect to temperature) is positive for the P1 and P2 products, thus reflecting an increase of the activation energy with temperature, while the opposite behavior (n negative) is obtained for P3. Finally, the value of the pre-exponential factor A is typical for this kind of reaction and rules the branching ratio between the different channels.

CONCLUSIONS

Astrochemistry and atmospheric chemistry require accurate kinetic data for processes occurring at low to moderate temperatures and involving barrier heights spanning a large range of values. Furthermore, the chemical species involved in these processes can contain more than 10 non-hydrogen atoms and noncovalent interactions may often rule the entrance channels. We have, therefore, developed and validated a new general model rooted in the master equation formalism employing the ab initio transition-state theory for computing the reaction rates of elementary processes. To this end, we have slightly modified and validated the recently proposed jChS model chemistry with reference to very accurate energetic and kinetic data. The results obtained for a large panel of systems and reaction channels show an average error within 0.3 kcal mol^{-1} without the need for any empirical parameter, which allows the evaluation of accurate branching ratios and leads to errors within 20% for reaction rates.

The computational bottleneck of the proposed model chemistry is the CCSD(T)/jun-cc-pVTZ step and, in this connection, recent localized treatments of correlation (e.g., using local pair natural orbitals[120,121]) will be investigated to further increase the dimension of molecular systems amenable to accurate computations with reasonable computer requirements. Furthermore, the performances of the jChS model for other classes of reactions of particular interest for astrochemistry and/or atmospheric chemistry (e.g., those involving ozone and Criegee intermediate) need be investigated in deeper detail. In the same vein, further refinements and validations are surely needed for specific situations (e.g., non-negligible static correlation effects or intersystem crossing). However, even taking these caveats into account, we think that the results reported in the present paper pave the route for the accurate study of chemical processes under widely different temperature and pressure conditions.

■ ASSOCIATED CONTENT

ⓢ Supporting Information

The Supporting Information is available free of charge at https://pubs.acs.org/doi/10.1021/acs.jctc.1c00406.

> Extended table of results for the HTBH38/08 data set, Cartesian coordinates of all of the stationary points optimized in this work, and MESS input files (PDF)

■ AUTHOR INFORMATION

Corresponding Author

Vincenzo Barone — *SMART Laboratory, Scuola Normale Superiore di Pisa, 56125 Pisa, Italy;* ⓞ orcid.org/0000-0001-6420-4107; Email: vincenzo.barone@sns.it

Authors

Jacopo Lupi — *SMART Laboratory, Scuola Normale Superiore di Pisa, 56125 Pisa, Italy;* ⓞ orcid.org/0000-0001-6522-9947

Zoi Salta — *SMART Laboratory, Scuola Normale Superiore di Pisa, 56125 Pisa, Italy;* ⓞ orcid.org/0000-0002-7826-0182

Nicola Tasinato — *SMART Laboratory, Scuola Normale Superiore di Pisa, 56125 Pisa, Italy;* ⓞ orcid.org/0000-0003-1755-7238

Complete contact information is available at:
https://pubs.acs.org/10.1021/acs.jctc.1c00406

Notes

The authors declare no competing financial interest.

■ ACKNOWLEDGMENTS

■ REFERENCES

(1) Woon, D. E. The Astrochymist. http://www.astrochymist.org/ (accessed Dec 5, 2018).

(2) Herbst, E.; van Dishoeck, F. E. Complex Organic Interstellar Molecules. *Annu. Rev. Astron. Astrophys.* **2009**, *47*, 427−480.

(3) Snow, T. P.; McCall, B. J. Diffuse Atomic and Molecular Clouds. *Annu. Rev. Astron. Astrophys.* **2006**, *44*, 367−414.

(4) Yamamoto, S. *Introduction to Astrochemistry*; Springer, 2017.

(5) Dobrijevic, M.; Loison, J. C.; Hickson, K. M.; Gronoff, G. 1D-coupled photochemical model of neutrals, cations and anions in the atmosphere of Titan. *Icarus* **2016**, *268*, 313−339.

(6) Carbo, R.; Ginebreda, A. Interstellar chemistry. *J. Chem. Educ.* **1985**, *62*, 832−836.

(7) Atkinson, R.; Baulch, D. L.; Cox, R. A.; Crowley, J. N.; Hampson, R. F.; Hynes, R. G.; Jenkin, M. E.; Rossi, M. J.; Troe, J.; IUPAC Subcommittee. Evaluated kinetic and photochemical data for atmospheric chemistry: Volume II - gas phase reactions of organic species. *Atmos. Chem. Phys.* **2006**, *6*, 3625−4055.

(8) Kwok, E. S.; Atkinson, R. Estimation of hydroxyl radical reaction rate constants for gas-phase organic compounds using a structure-reactivity relationship: An update. *Atmos. Environ.* **1995**, *29*, 1685−1695.

(9) Vereecken, L.; Glowacki, D. R.; Pilling, M. J. Theoretical chemical kinetics in tropospheric chemistry: methodologies and applications. *Chem. Rev.* **2015**, *115*, 4063−4114.

(10) Karton, A. A computational chemist's guide to accurate thermochemistry for organic molecules. *WIREs Comput. Mol. Sci.* **2016**, *6*, 292−310.

(11) Karton, A.; Martin, J. M. L. Explicitly correlated Wn theory: W1-F12 and W2-F12. *J. Chem. Phys.* **2012**, *136*, No. 124114.

(12) Laane, J.; Dakkouri, M.; van der Veken, B.; Oberhammer, H. *Structures and Conformations of Non-Rigid Molecules*; Springer: Netherlands, 1993; Vol. *410*.

(13) Császár, A. G.; Allen, W. D.; Schaefer, H. F. In pursuit of the ab initio limit for conformational energy prototypes. *J. Chem. Phys.* **1998**, *108*, 9751−9764.

(14) Peterson, K. A.; Feller, D.; Dixon, D. A. Chemical accuracy in ab initio thermochemistry and spectroscopy: Current strategies and future challenges. *Theor. Chem. Acc.* **2012**, *131*, 1−50.

(15) Tajti, A.; Szalay, P. G.; Császár, A. G.; Kállay, M.; Gauss, J.; Valeev, E. F.; Flowers, B. A.; Vázquez, J.; Stanton, J. F. HEAT: High accuracy extrapolated ab initio thermochemistry. *J. Chem. Phys.* **2004**, *121*, 11599−11613.

(16) Bomble, Y. J.; Vázquez, J.; Kállay, M.; Michauk, C.; Szalay, P. G.; Császár, A. G.; Gauss, J.; Stanton, J. F. High-accuracy extrapolated ab initio thermochemistry. II. Minor improvements to the protocol and a vital simplification. *J. Chem. Phys.* **2006**, *125*, No. 064108.

(17) Harding, M. E.; Vázquez, J.; Ruscic, B.; Wilson, A. K.; Gauss, J.; Stanton, J. F. High-accuracy extrapolated ab initio thermochemistry. III. Additional improvements and overview. *J. Chem. Phys.* **2008**, *128*, No. 114111.

(18) Zhang, J.; Valeev, E. F. Prediction of reaction barriers and thermochemical properties with explicitly correlated coupled-cluster methods: a basis set assesment. *J. Chem. Theory Comput.* **2012**, *8*, 3175−3186.

(19) Curtiss, L. A.; Redfern, P. C.; Raghavachari, K. Gn theory. *WIREs Comput. Mol. Sci.* **2011**, *1*, 810−825.

(20) Curtiss, A. L.; Redfern, C. P.; Raghavachari, K. Gaussian-4 theory. *J. Chem. Phys.* **2007**, *126*, No. 084108.

(21) Montgomery, J. A.; Ochterski, J. W.; Petersson, G. CBS. *J. Chem. Phys.* **1994**, *101*, 5900−5909.

(22) Montgomery, J. A.; Frisch, M. J.; Ochterski, J. W.; Petersson, G. A. A complete basis set model chemistry. VII. Use of the minimum population localization method. *J. Chem. Phys.* **2000**, *112*, 6532−6542.

(23) Curtiss, L. A.; Redfern, P. C.; Raghavachari, K. Assessment of Gaussian-4 theory for energy barriers. *Chem. Phys. Lett.* **2010**, *499*, 168−172.

(24) Puzzarini, C.; Barone, V. Extending the molecular size in accurate quantum-chemical calculations: the equilibrium structure and spectroscopic properties of uracil. *Phys. Chem. Chem. Phys.* **2011**, *13*, 7189−7197.

(25) Puzzarini, C.; Biczysko, M.; Barone, V.; Peña, I.; Cabezas, C.; Alonso, J. L. Accurate molecular structure and spectroscopic

properties of nucleobases: a combined computational-microwave investigation of 2-thiouracil as a case study. *Phys. Chem. Chem. Phys.* **2013**, *15*, 16965−16975.

(26) Puzzarini, C.; Biczysko, M.; Barone, V.; Largo, L.; Peña, I.; Cabezas, C.; Alonso, J. L. Accurate Characterization of the Peptide Linkage in the Gas Phase: a Joint Quantum-chemical and Rotational Spectroscopy Study of the Glycine Dipeptide Analogue. *J. Phys. Chem. Lett.* **2014**, *5*, 534−540.

(27) Salta, Z.; Tasinato, N.; Lupi, J.; Boussessi, R.; Balbi, A.; Puzzarini, C.; Barone, V. Exploring the Maze of $C_2N_2H_5$ Radicals and Their Fragments in the Interstellar Medium with the Help of Quantum-Chemical Computations. *ACS Earth Space Chem.* **2020**, *4*, 774−782.

(28) Lupi, J.; Puzzarini, C.; Cavallotti, C.; Barone, V. State-of-the-Art Quantum Chemistry Meets Variable Reaction Coordinate Transition State Theory to Solve the Puzzling Case of the H_2S + Cl System. *J. Chem. Theory Comput.* **2020**, *16*, 5090−5104.

(29) Lupi, J.; Puzzarini, C.; Barone, V. Methanimine as a Key Precursor of Imines in the Interstellar Medium: The Case of Propargylimine. *Astrophys. J. Lett.* **2020**, *903*, No. L35.

(30) Baiano, C.; Lupi, J.; Tasinato, N.; Puzzarini, C.; Barone, V. The Role of State-of-the-Art Quantum-Chemical Calculations in Astrochemistry: Formation Route and Spectroscopy of Ethanimine as a Paradigmatic Case. *Molecules* **2020**, *25*, No. 2873.

(31) Ballotta, B.; Nandi, S.; Barone, V.; Rampino, S. Gas-Phase Formation and Isomerization Reactions of Cyanoacetaldehyde, a Prebiotic Molecule of Astrochemical Interest. *ACS Earth Space Chem.* **2021**, *5*, 1071−1082.

(32) Papajak, E.; Zheng, J.; Xu, X.; Leverentz, R. H.; Truhlar, G. D. Perspectives on Basis Sets Beautiful: Seasonal Plantings of Diffuse Basis Functions. *J. Chem. Theory Comput.* **2011**, *7*, 3027−3034.

(33) Alessandrini, S.; Barone, V.; Puzzarini, C. Extension of the "Cheap" Composite Approach to Noncovalent Interactions: The jun-ChS Scheme. *J. Chem. Theory Comput.* **2020**, *16*, 988−1006.

(34) Melli, A.; Barone, V.; Puzzarini, C. Unveiling Bifunctional Hydrogen Bonding with the Help of Quantum Chemistry: The Imidazole-Water Adduct as Test Case. *J. Phys. Chem. A* **2021**, *125*, 2989−2998.

(35) Bao, J. L.; Truhlar, D. G. Variational transition state theory: theoretical framework and recent developments. *Chem. Soc. Rev.* **2017**, *46*, 7548−7596.

(36) Miller, A. J.; Klippenstein, J. S. Master equation methods in gas phase chemical kinetics. *J. Phys. Chem. A* **2006**, *110*, 10528−10544.

(37) Klippenstein, S. J. From Theoretical Reaction Dynamics to Chemical Modeling of Combustion. *Proc. Combust. Inst.* **2017**, *36*, 77−111.

(38) Zheng, J.; Zhao, Y.; Truhlar, D. G. The DBH24/08 Database and Its Use to Assess Electronic Structure Model Chemistries for Chemical Reaction Barrier Heights. *J. Chem. Theory Comput.* **2009**, *5*, 808−821.

(39) Zhao, Y.; Lynch, B. J.; Truhlar, D. G. Multi-coefficient extrapolated density functional theory for thermochemistry and thermochemical kinetics. *Phys. Chem. Chem. Phys.* **2005**, *7*, 43−52.

(40) Zhao, Y.; González-García, N.; Truhlar, D. G. Benchmark Database of Barrier Heights for Heavy Atom Transfer, Nucleophilic Substitution, Association, and Unimolecular Reactions and Its Use to Test Theoretical Methods. *J. Phys. Chem. A* **2005**, *109*, 2012−2018.

(41) Karton, A. Highly Accurate CCSDT(Q)/CBS Reaction Barrier Heights for a Diverse Set of Transition Structures: Basis Set Convergence and Cost-Effective Approaches for Estimating Post-CCSD(T) Contributions. *J. Phys. Chem. A* **2019**, *123*, 6720−6732.

(42) Karton, A.; Rabinovich, E.; Martin, J. M. L.; Ruscic, B. W4 theory for computational thermochemistry: In pursuit of confident sub-kJ/mol predictions. *J. Chem. Phys.* **2006**, *125*, No. 144108.

(43) Dunning, T. H., Jr. Gaussian basis sets for use in correlated molecular calculations. I. The atoms boron through neon and hydrogen. *J. Chem. Phys.* **1989**, *90*, 1007−1023.

(44) Raghavachari, K.; Trucks, G. W.; Pople, J. A.; Head-Gordon, M. A fifth-order perturbation comparison of electron correlation theories. *Chem. Phys. Lett.* **1989**, *157*, 479−483.

(45) Møller, C.; Plesset, M. S. Note on an Approximation Treatment for Many-Electron Systems. *Phys. Rev.* **1934**, *46*, 618−622.

(46) Sellers, H.; Pulay, P. The adiabatic correction to molecular potential surfaces in the SCF approximation. *Chem. Phys. Lett.* **1984**, *103*, 463−465.

(47) Handy, N. C.; Yamaguchi, Y.; Schaefer, H. F. The diagonal correction to the Born-Oppenheimer approximation: Its effect on the singlet-triplet splitting of CH_2 and other molecular effects. *J. Chem. Phys.* **1986**, *84*, 4481−4484.

(48) Handy, N. C.; Lee, A. M. The adiabatic approximation. *Chem. Phys. Lett.* **1996**, *252*, 425−430.

(49) Kutzelnigg, W. The adiabatic approximation I. The physical background of the Born-Handy ansatz. *Mol. Phys.* **1997**, *90*, 909−916.

(50) Cowan, R. D.; Griffin, M. Approximate relativistic corrections to atomic radial wave functions. *J. Opt. Soc. Am.* **1976**, *66*, 1010−1014.

(51) Martin, R. L. All-electron relativistic calculations on silver hydride. An investigation of the Cowan-Griffin operator in a molecular species. *J. Phys. Chem. A* **1983**, *87*, 750−754.

(52) Bomble, Y. J.; Stanton, J. F.; Kállay, M.; Gauss, J. Coupled-cluster methods including noniterative corrections for quadruple excitations. *J. Chem. Phys.* **2005**, *123*, No. 054101.

(53) Kállay, M.; Gauss, J. Approximate treatment of higher excitations in coupled-cluster theory. *J. Chem. Phys.* **2005**, *123*, No. 214105.

(54) Kállay, M.; Gauss, J. Approximate treatment of higher excitations in coupled-cluster theory. II. Extension to general single-determinant reference functions and improved approaches for the canonical Hartree−Fock case. *J. Chem. Phys.* **2008**, *129*, No. 144101.

(55) Moore, C. E. Atomic Energy Levels; Natl. Bur. Stand. (US) Circ., 1949.

(56) Santra, G.; Sylvetsky, N.; Martin, J. M. Minimally empirical double-hybrid functionals trained against the GMTKN55 database: revDSD-PBEP86-D4, revDOD-PBE-D4, and DOD-SCAN-D4. *J. Phys. Chem. A* **2019**, *123*, 5129−5143.

(57) Biczysko, M.; Panek, P.; Scalmani, G.; Bloino, J.; Barone, V. Harmonic and Anharmonic Vibrational Frequency Calculations with the Double-Hybrid B2PLYP Method: Analytic Second Derivatives and Benchmark Studies. *J. Chem. Theory Comput.* **2010**, *6*, 2115−2125.

(58) Barone, V. Anharmonic vibrational properties by a fully automated second order perturbative approach. *J. Chem. Phys.* **2005**, *122*, No. 014108.

(59) Barone, V.; Biczysko, M.; Bloino, J. Fully anharmonic IR and Raman spectra of medium-size molecular systems: accuracy and interpretation. *Phys. Chem. Chem. Phys.* **2014**, *16*, 1759−1787.

(60) Frisch, M. J. et al. *Gaussian 16*, revision C.01; Gaussian Inc.: Wallingford CT, 2016.

(61) Werner, H.-J.; et al. The Molpro quantum chemistry package. *J. Chem. Phys.* **2020**, *152*, No. 144107.

(62) Kállay, M. et al. MRCC, a quantum chemical program suite, 2018.

(63) Stanton, J. F.; Gauss, J.; Harding, M. E.; Szalay, P. G. A quantum chemical program package. 2016; with contributions from Auer, A. A.; Bartlett, R. J.; Benedikt, U.; Berger, C.; Bernholdt, D. E.; Bomble, Y. J.; Christiansen, O.; Engel, F.; Heckert, M.; Heun, O.; Huber, C.; Jagau, T.-C.; Jonsson, D.; Jusèlius, J.; Klein, K.; Lauderdale, W. J.; Lipparini, F.; Matthews, D.; Metzroth, T.; Mück, L. A.; O'Neill, D. P.; Price, D. R.; Prochnow, E.; Puzzarini, C.; Ruud, K.; Schiffmann, F.; Schwalbach, W.; Stopkowicz, S.; Tajti, A.; Vázquez, J.; Wang, F.; Watts, J. D., and the integral packages MOLECULE (J. Almlöf and P. R. Taylor), PROPS (P. R. Taylor), ABACUS (T. Helgaker, H. J. Aa. Jensen, P. Jørgensen, and J. Olsen), and ECP routines by A. V. Mitin and C. van Wüllen. For the current version, see http://www.cfour.de.

(64) Woon, D. E.; Dunning, T. H., Jr. Gaussian Basis Sets for Use in Correlated Molecular Calculations. V. Core-Valence Basis Sets for Boron through Neon. *J. Chem. Phys.* **1995**, *103*, 4572–4585.

(65) Feller, D. Application of systematic sequences of wave functions to the water dimer. *J. Chem. Phys.* **1992**, *96*, 6104–6114.

(66) Helgaker, T.; Klopper, W.; Koch, H.; Noga, J. Basis-set convergence of correlated calculations on water. *J. Chem. Phys.* **1997**, *106*, 9639–9646.

(67) Georgievskii, Y.; Miller, A. J.; Burke, P. M.; Klippenstein, J. S. Reformulation and solution of the master equation for multiple-well chemical reactions. *J. Phys. Chem. A* **2013**, *117*, 12146–12154.

(68) Tardy, D. C.; Rabinovitch, B. Collisional Energy Transfer. Thermal Unimolecular Systems in the Low-Pressure Region. *J. Chem. Phys.* **1966**, *45*, 3720–3730.

(69) Fernández-Ramos, A.; Miller, J. A.; Klippenstein, S. J.; Truhlar, D. G. Modeling the Kinetics of Bimolecular Reactions. *Chem. Rev.* **2006**, *106*, 4518–4584.

(70) Eckart, C. The penetration of a potential barrier by electrons. *Phys. Rev.* **1930**, *35*, 1303–1309.

(71) Hunter, M.; Reid, S. A.; Robie, D. C.; Reisler, H. The Monoenergetic Unimolecular Reaction of Expansion-Cooled NO_2: NO Product State Distributions at Excess Energies 0–3000 cm^{-1}. *J. Chem. Phys.* **1993**, *99*, 1093–1108.

(72) Skouteris, D.; Balucani, N.; Ceccarelli, C.; Vazart, F.; Puzzarini, C.; Barone, V.; Codella, C.; Lefloch, B. The Genealogical Tree of Ethanol: Gas-phase Formation of Glycolaldehyde, Acetic Acid, and Formic Acid. *Astrophys. J.* **2018**, *854*, No. 135.

(73) Kooij, D. M. *Z. Phys. Chem.* **1893**, *12*, 155–161.

(74) Laidler, K. J. A glossary of terms used in chemical kinetics, including reaction dynamics (IUPAC recommendations 1996). *Pure Appl. Chem.* **1996**, *68*, 149–192.

(75) Grimme, S. Semiempirical hybrid density functional with perturbative second-order correlation. *J. Chem. Phys.* **2006**, *124*, No. 034108.

(76) Grimme, S. Density functional theory with London dispersion corrections. *WIREs Comput. Mol. Sci.* **2011**, *1*, 211–228.

(77) Caldeweyher, E.; Bannwarth, C.; Grimme, S. Extension of the D3 dispersion coefficient model. *J. Chem. Phys.* **2017**, *147*, No. 034112.

(78) Xie, F.; Fusè, M.; Hazrah, A. S.; Jaeger, W.; Barone, V.; Xu, Y. Discovering the elusive global minimum in a ternary chiral cluster: rotational spectra of propylene oxide trimer. *Angew. Chem., Int. Ed.* **2020**, *59*, 22427–22430.

(79) Alonso, E. R.; Fusè, M.; León, I.; Puzzarini, C.; Alonso, J. L.; Barone, V. Exploring the maze of cycloserine conformers in the gas phase guided by microwave spectroscopy and quantum chemistry. *J. Phys. Chem. A* **2021**, *125*, 2121–2129.

(80) Barone, V.; Ceselin, G.; Fusè, M.; Tasinato, N. Accuracy Meets Interpretability for Computational Spectroscopy by Means of Hybrid and Double-Hybrid Functionals. *Front. Chem.* **2020**, *8*, 584203-1–584203-14.

(81) Sosa, C.; Schlegel, H. B. Ab initio calculations on the barrier height for the hydrogen addition to ethylene and formaldehyde. The importance of spin projection. *Int. J. Quantum Chem.* **1986**, *29*, 1001–1015.

(82) Schlegel, H. B. Møller-Plesset Perturbation Theory with Spin Projection. *J. Phys. Chem. A* **1988**, *92*, 3075–3378.

(83) Yuan, H.; Cremer, D. The expectation value of the spin operator S^2 as a diagnostic tool in coupled cluster theory. The advantages of using UHF-CCSD theory for the description of homolytic dissociation. *Chem. Phys. Lett.* **2000**, *324*, 389–402.

(84) Stanton, J. F. On the extent of spin contamination in open-shell coupled-cluster wave functions. *J. Chem. Phys.* **1994**, *101*, 371–374.

(85) Cohen, A. J.; Tozer, D. J.; Handy, N. C. Evaluation of S^2 in density functional theory. *J. Chem. Phys.* **2007**, *126*, No. 214104.

(86) Menon, A. S.; Radom, L. Consequences of Spin Contamination in Unrestricted Calculations on Open-Shell Species: Effect of Hartree Fock and Møller Plesset Contributions in Hybrid and Double-Hybrid Density Functional Theory Approaches. *J. Phys. Chem. A* **2008**, *112*, 13225–13230.

(87) Karton, A.; Tarnopolsky, A.; Lamère, J.; Schatz, G. C.; Martin, J. M. L. Highly Accurate First-Principles Benchmark Data Sets for the Parametrization and Validation of Density Functional and Other Approximate Methods. Derivation of a Robust, Generally Applicable, Double-Hybrid Functional for Thermochemistry and Thermochemical Kinetics. *J. Phys. Chem. A* **2008**, *112*, 12868–12886.

(88) Karton, A.; Rabinovich, E.; Martin, J. M. L.; Ruscic, B. W4 Theory for computational thermochemistry: in pursuit of confident sub-kJ/mol predictions. *J. Chem. Phys.* **2011**, *125*, No. 144108.

(89) Kong, L.; Bischoff, F. A.; Valeev, E. F. Explicitly Correlated R12/F12 Methods for Electronic Structure. *Chem. Rev.* **2012**, *112*, 75–107.

(90) Guner, V.; Khuong, K. S.; Leach, A. G.; Lee, P. S.; Bartberger, M. D.; Houk, K. N. A Standard Set of Pericyclic Reactions of Hydrocarbons for the Benchmarking of Computational Methods: The Performance of ab Initio, Density Functional, CASSCF, CASPT2, and CBS-QB3 Methods for the Prediction of Activation Barriers, Reaction Energetics, and Transition State Geometries. *J. Phys. Chem. A* **2003**, *107*, 11445–11459.

(91) Karton, A.; Goerigk, L. Accurate reaction barrier heights of pericyclic reactions: Surprisingly large deviations for the CBS-QB3 composite method and their consequences in DFT benchmark studies. *J. Comput. Chem* **2015**, *36*, 622–632.

(92) Yu, L.-J.; Sarrami, F.; O'Reilly, R. J.; Karton, A. Reaction barrier heights for cycloreversion of heterocyclic rings: An Achilles' heel for DFT and standard ab initio procedures. *Chem. Phys.* **2015**, *458*, 1–8.

(93) Ess, D. H.; Houk, K. N. Activation Energies of Pericyclic Reactions: Performance of DFT, MP2, and CBS-QB3 Methods for the Prediction of Activation Barriers and Reaction Energetics of 1,3-Dipolar Cycloadditions, and Revised Activation Enthalpies for a Standard Set of Hydrocarbon Pericyclic Reactions. *J. Phys. Chem. A* **2005**, *109*, 9542–9553.

(94) Karton, A.; O'Reilly, R. J.; Chan, B.; Radom, L. Determination of Barrier Heights for Proton Exchange in Small Water, Ammonia, and Hydrogen Fluoride Clusters with G4(MP2)-Type, MPn, and SCS-MPn Procedures–A Caveat. *J. Chem. Theory Comput.* **2012**, *8*, 3128–3136.

(95) Goerigk, L.; Hansen, A.; Bauer, C.; Ehrlich, S.; Najibi, A.; Grimme, S. A look at the density functional theory zoo with the advanced GMTKN55 database for general main group thermochemistry, kinetics and noncovalent interactions. *Phys. Chem. Chem. Phys.* **2017**, *19*, 32184–32215.

(96) Irikura, K. K.; Johnson, R.; Kacker, R. N.; Kessel, R. Uncertainties in scaling factors for ab initio vibrational zero-point energies. *J. Chem. Phys.* **2009**, *130*, No. 114102.

(97) Kesharwani, M. K.; Brauer, B.; Martin, J. M. L. Frequency and Zero-Point Vibrational Energy Scale Factors for Double-Hybrid Density Functionals (and Other Selected Methods): Can Anharmonic Force Fields Be Avoided? *J. Phys. Chem. A* **2015**, *119*, 1701–1714.

(98) Skouteris, D.; Calderini, D.; Barone, V. Methods for calculating partition functions of molecules involving large amplitude and/or anharmonic motions. *J. Chem. Theory Comput.* **2016**, *12*, 1011–1018.

(99) Schuurman, M. S.; Allen, W. D.; von Raguè Schleyer, P.; Schaefer, H. F. I. The highly anharmonic BH5 potential energy surface characterized in the ab initio limit. *J. Chem. Phys.* **2005**, *122*, No. 104302.

(100) Piccardo, M.; Bloino, J.; Barone, V. Generalized vibrational perturbation theory for rotovibrational energies of linear, symmetric and asymmetric tops: Theory, approximations, and automated approaches to deal with medium-to-large molecular systems. *Int. J. Quantum Chem.* **2015**, *115*, 948–982.

(101) Bloino, J.; Biczysko, M.; Barone, V. General perturbative approach for spectroscopy, thermodynamics and kinetics: methodological background and benchmark studies. *J. Chem. Theory Comput.* **2012**, *8*, 1015–1036.

(102) Ayala, P. Y.; Schlegel, H. B. Identification and treatment of internal rotation in normal mode vibrational analysis. *J. Phys. Chem. A* **1998**, *108*, 2314−2325.

(103) Truhlar, D. G.; Isaacson, A. D. Simple perturbation theory estimates of equilibrium constants from force fields. *J. Chem. Phys.* **1991**, *94*, 357−359.

(104) Afeefy, H. Y.; Liebman, J. F.; Stein, S. E. In *NIST Chemistry WebBook, NIST Standard Reference Database Number 69*; Linstrom, P. J.; Mallard, W. G., Eds.; National Institute of Standards and Technology: Gaithersburg, MD, 2021; Chapter Neutral Thermochemical Data.

(105) Harding, L. B.; Georgievskii, Y.; Klippenstein, S. J. Accurate anharmonic zero-point energies for some combustion-related species from diffusion Monte Carlo. *J. Phys. Chem. A* **2017**, *121*, 4334−4340.

(106) Avila, G.; Carrington, T. J. Using a pruned basis, a non-product quadrature grid, and the exact Watson normal-coordinate kinetic energy operator to solve the vibrational Schrödinger equation for C2H4. *J. Chem. Phys.* **2011**, *135*, No. 064101.

(107) Li, Y.-P.; Bell, A. T.; Head-Gordon, M. Thermodynamics of anharmonic systems: uncoupled mode approximations for molecules. *J. Chem. Theory Comput.* **2016**, *12*, 2861−2870.

(108) Chandramouli, B.; Del Galdo, S.; Fuse, M.; Barone, V.; Mancini, G. Two-level strochastic search of low-energy conformers for molecular spectroscopy: implementation and validation of MM and QM models. *Phys. Chem. Chem. Phys.* **2019**, *21*, 19921−19934.

(109) Mancini, G.; Fuse, M.; Lazzari, F.; Chandramouli, B.; Barone, V. Unsupervised search of low-lying conformers with spectroscopic accuracy: a two-step algorithm rooted into the island model evolutionary algorithm. *J. Chem. Phys.* **2020**, *153*, No. 124110.

(110) Puzzarini, C.; Bloino, J.; Tasinato, N.; Barone, V. Accuracy and interpretability: The devil and the holy grail. New routes across old boundaries in computational spectroscopy. *Chem. Rev.* **2019**, *119*, 8131−8191.

(111) Chao, J.; Hall, K. R.; Marsh, K. N.; Wilhoit, R. C. Thermodynamic Properties of Key Organic Oxygen Compounds in the Carbon Range C1 to C4. Part 2. Ideal Gas Properties. *J. Phys. Chem. Ref. Data* **1986**, *15*, 1369−1436.

(112) Dorofeeva, O.; Novikov, V. P.; Neumann, D. B. NIST-JANAF Thermochemical Tables. I. Ten Organic Molecules Related to Atmospheric Chemistry. *J. Phys. Chem. Ref. Data* **2001**, *30*, 475−513.

(113) Ruscic, B.; Boggs, J. E.; Burcart, A.; Császár, A.; Demaison, J.; Janoshek, R.; Martin, J. M. l.; Morton, M. L.; Rossi, M. J.; Stanton, J. F.; Szalas, P. G.; Westmoreland, P. R.; Zabel, F.; Berces, T. IUPAC critical evaluation of thermodynamical properties of selected radicals. Part I. *J. Phys. Chem. Ref. Data* **2005**, *34*, 573−656.

(114) Demaison, J.; Margulès, L.; Boggs, J. E. Equilibrium structure and force field of NH$_2$. *Phys. Chem. Chem. Phys.* **2003**, *5*, 3359−3363.

(115) Marenich, A. V.; Boggs, J. E. Coupled cluster CCSD(T) calculations of equilibrium geometries, anharmonic force fields, and thermodynamic properties of formyl (HCO) and isoformyl (HOC) radical species. *J. Phys. Chem. A* **2003**, *107*, 2343−2350.

(116) Vichietti, R. M.; Machado, F. B.; Haiduke, L. A. Accurate rate constants for the forward and reverso H$^{\bullet}$ + CO → HCO$^{\bullet}$ reactions at the high-pressure limit. *ACS Omega* **2020**, *5*, 23975−23982.

(117) Sleiman, C.; El Dib, G.; Rosi, M.; Skouteris, D.; Balucani, N.; Canosa, A. Low temperature kinetics and theoretical studies of the reaction CN + CH3NH2: a potential source of cyanamide and methyl cyanamide in the interstellar medium. *Phys. Chem. Chem. Phys.* **2018**, *20*, 5478−5489.

(118) Puzzarini, C.; Salta, Z.; Tasinato, N.; Lupi, J.; Cavallotti, C.; Barone, V. A twist on the reaction of the CN radical with methylamine in the interstellar medium: new hints from a state-of-the-art quantum-chemical study. *Mon. Not. R. Astron. Soc.* **2020**, *496*, 4298−4310.

(119) Simmie, J. M.; Somers, K. P. Benchmarking Compound Methods (CBS-QB3, CBS-APNO, G3, G4, W1BD) against the Active Thermochemical Tables: A Litmus Test for Cost-Effective Molecular Formation Enthalpies. *J. Phys. Chem. A* **2015**, *119*, 7235−7246.

(120) Nagy, P. R.; Kallay, M. Approaching the basis set limit of CCSD(T) energies for large molecules with local natural orbital coupled-cluster methods. *J. Chem. Theory Comput.* **2019**, *15*, 5275−5298.

(121) Liakos, D. G.; Guo, Y.; Neese, F. Comprehensive benchmark results for the domain based local pair natural orbital coupled cluster method (DLPNO-CCSD(T)) for closed- and open-shell systems. *J. Phys. Chem. A* **2020**, *124*, 90−100.